

# For Reference

---

NOT TO BE TAKEN FROM THIS ROOM



# For Reference

NOT TO BE TAKEN FROM THIS ROOM

Ex LIBRIS  
UNIVERSITATIS  
ALBERTAENSIS







Thesis  
1963  
# 41

THE UNIVERSITY OF ALBERTA

TRANSPORT PROPERTIES OF SOME  
RESISTANCE-MINIMUM ALLOYS

by

W. T. MacFARLANE

A THESIS

SUBMITTED TO THE FACULTY OF GRADUATE STUDIES  
IN PARTIAL FULFILMENT OF THE REQUIREMENTS FOR THE  
DEGREE OF MASTER OF SCIENCE

DEPARTMENT OF PHYSICS

EDMONTON, ALBERTA

APRIL 19, 1963.

THE  
UNIVERSITY OF  
THE SOUTH ALABAMA  
LIBRARY

THE  
UNIVERSITY OF  
THE SOUTH ALABAMA  
LIBRARY

THE  
UNIVERSITY OF  
THE SOUTH ALABAMA  
LIBRARY

THE  
UNIVERSITY OF  
THE SOUTH ALABAMA  
LIBRARY

UNIVERSITY OF ALBERTA  
FACULTY OF GRADUATE STUDIES

The undersigned certify that they have read,  
and recommend to the Faculty of Graduate Studies for  
acceptance, a thesis entitled Transport Properties of  
Some Resistance-Minimum Alloys submitted by W. T.  
MacFarlane in partial fulfilment of the requirements for  
the degree of Master of Science.





## TABLE OF CONTENTS

ACKNOWLEDGEMENTS	
ABSTRACT	
INTRODUCTION	1
PART 1 THEORY	
1.1 Historical Review	6
1.2 The Electrical Resistivity	14
1.3 The Electron Thermal Conductivity	15
1.4 The Lattice Conductivity	16
PART 2 EXPERIMENTAL WORK	
2.1 General	17
2.2 The Gas Thermometers	21
2.3 The Galvanometer Amplifier	25
2.4 Specimen Preparation	27
a) Preliminary	27
b) Preparation of the Alloys	28
c) Drawing and Annealing	30
d) Specimen Purity	30
e) Specimen Mounting	31
2.5 The Resistance - Wound Furnace	33
2.6 The Magnetic Field	36
2.7 Experimental Procedure	36
PART 3 RESULTS	
3.1 Experimental Results	38
3.2 Conclusions	50
APPENDIX	53
SAMPLE CALCULATION	53
REFERENCES	55



Digitized by the Internet Archive  
in 2019 with funding from  
University of Alberta Libraries

<https://archive.org/details/MacFarlane1963>

## LIST OF ILLUSTRATIONS

Figure 1.	Electrical Resistivity of Copper	3
Figure 2.	The Fermi Surface of Copper	9
Figure 3.	The Cryostat in the Magnet	18
Figure 4.	The Gas Thermometers	22
Figure 5.	Gas Thermometer Corrections	24
Figure 6.	Dendrites in 4% Copper-iron Alloy	29
Figure 7.	The Resistance-wound Furnace	33
Figure 8.	Specimen Chamber	34
Figure 9.	Temperature Distribution Curves of Furnace	35
Figure 10.	The magnetic Field	37
Figure 11.	Electrical Resistivity of Pure Copper and Alloys	39
Figure 12.	Thermal Conductivity of Copper + 0.015% Iron Alloy	41
Figure 13.	Thermal Conductivity of Copper + 0.127% Iron Alloy	43
Figure 14.	Electrical Magnetoresistance at 2 °K	45
Figure 15.	Electrical Magnetoresistance at 4 °K	46
Figure 16.	Thermal Magnetoresistance	47
Figure 17.	Magnetoresistance at 8 °K	48
Figure 18.	Electrical Magnetoresistance	49





## ACKNOWLEDGEMENTS

I wish to thank Dr. S. B. Woods, my research supervisor, for suggesting this project and for his help throughout the course of this research.

I also wish to thank the members of the staff of the Department of Mining and Metallurgy for much help and for the use of some of their facilities from time to time.

The financial support of this project by the National Research Council was greatly appreciated.

Finally, I would like to thank the members of the technical staff who assisted on numerous occasions.



## ABSTRACT

This thesis describes experiments performed to determine the electrical resistivity and the thermal conductivity of dilute copper-iron alloys at low temperatures. The experiments were performed on polycrystalline rods with solute concentrations up to 0.127 atomic percent iron. No change in the thermal conductivity associated with the well-known electrical resistivity minimum was found. The difficulty in detecting anomalies in the thermal conductivity is due to the increased importance of the lattice conductivity. Electrical and thermal magnetoresistivities were also measured in fields up to 15 k-oersted. The magnetoresistivities were found to decrease with increased solute concentration.





## INTRODUCTION

The electrical resistivity of a normal metal may be written according to Matthiessen's rule  $\rho(T) = \rho_0 + \rho_i(T)$  where  $\rho_0$  is the residual resistivity due to the static imperfections in the periodic potential and  $\rho_i(T)$  is the ideal resistivity due to scattering of the electrons by phonons of frequency,  $\nu$ , carrying energy,  $h\nu$ . At low temperatures  $\rho_i \ll \rho_0$  and the resistivity becomes constant as shown by the curve AB in Figure 1. The transport properties of dilute metal alloys at low temperatures have been observed to exhibit several striking variations from the normal behavior. The resistance minimum of the copper-iron alloys, the minimum and subsequent maximum at lower temperatures in the electrical resistance of the copper-manganese alloys and the "giant" thermoelectric power of these alloys are just a few of several examples. These anomalies are, in general due to a magnetic ion solute in the noble metal solvent. A magnetic ion is one such as a transition metal ion, with a large magnetic moment due to the irregular distribution of the extranuclear electrons. There is ample evidence for similar behavior in alloys with germanium, tin and other solutes but the present opinion is that these metals reduce the magnetic ions into the lattice from oxides which are not soluble in the parent metal but may instead be



segregated at the grain boundaries. Reasons for this present opinion are based on the fact that the size of the anomalies does not change with the addition of these solutes beyond very small concentrations (Gold et al (1960)). Below a temperature,  $T_{\min}$ , the electrical resistivity of the copper-iron alloys is observed to increase as the temperature is lowered as shown in the curve CD in Figure 1.

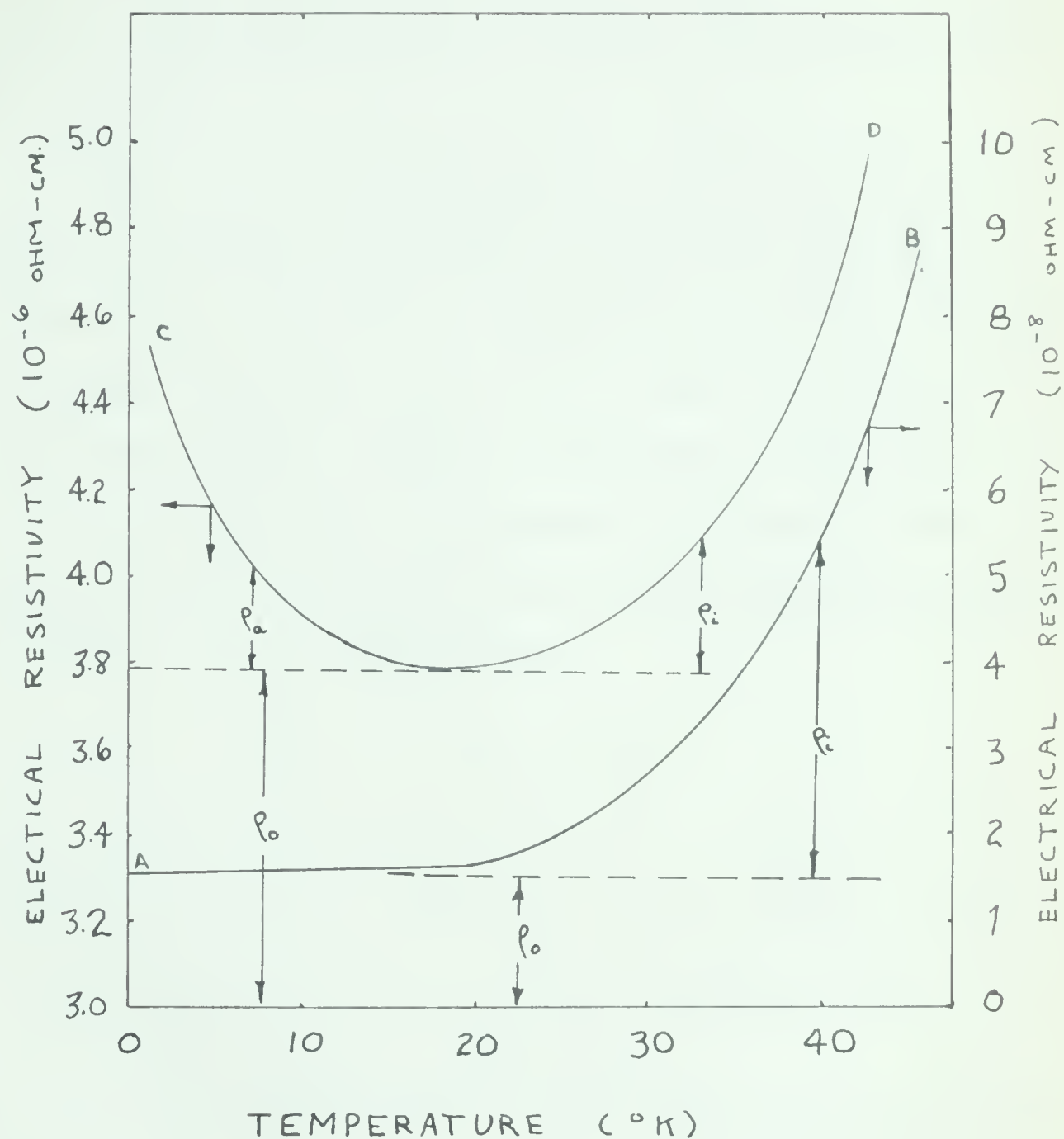
Now we might expect a corresponding change in the thermal conductivity but none had been observed in the few measurements previously made (White and Woods (1955)). It was of interest therefore to make a systematic survey of the low temperature thermal conductivity of a series of copper-iron alloys.

The thermal conductivity of a metal can be expressed as the sum of an electron and a lattice component. In pure metals the lattice conductivity is a very small part of the total but in alloys the electron and lattice conductivities often become comparable because the electron component is severely limited through the scattering of the electrons by irregularities in the lattice. A peculiar variation of the thermal conductivity with temperature has been observed in silver-manganese alloys at helium temperatures and is discussed by Chari (1961) and Chari and deNobel (1959). They attribute their observations to a partial uncoupling





Figure 1 . Electrical Resistivity of Copper (AB) and Copper-iron (CD): Schematic



- $\rho_0$  - Residual resistivity
- $\rho_i$  - Ideal resistivity
- $\rho_a$  - Anomalous resistivity



of the longitudinal and transverse phonons with a consequent effect on the lattice conductivity. This explanation was based on the experimental observation that the temperature variation of the conductivity was not significantly changed when the alloys were placed in strong (25 kilo-oersted) magnetic fields.

Another anomaly occurs in the variation of the electrical resistance of dilute noble metal alloys in a magnetic field. For normal metals at low fields the magnetoresistance is positive. However in copper-manganese alloys the magnetoresistance, shown by Gerritsen (1953) is negative, that is, the resistance decreases as the field rises, and it depends on the temperature and concentration of manganese in the alloy. Chari has written

$$K_H = L \sigma_H T + K_g$$

where  $K_H$  is the thermal conductivity in a magnetic field,

$K_g$  is the lattice component of the thermal conductivity,

$\sigma_H$  is the electrical conductivity in a magnetic field,

$T$  is the absolute temperature,

and  $L$  is the Lorenz number. The ratio  $K/\sigma T$  is called the Lorenz number and for a Fermi gas  $L = 2.45 \times 10^{-8}$  watt-ohm/degree<sup>2</sup>. Chari has shown that the Lorenz number for the silver-manganese alloys approaches this value at low temperature.





There are no published values for the magnetoresistance of copper-iron alloys although it was thought to be positive. We performed magnetoresistance measurements to test this hypothesis and, if possible, to help analyse the thermal conductivity data in a similar fashion to that used by Chari. This thesis describes the preparation of the alloys, the measurements of thermal and electrical conductivity both in and out of magnetic fields, and some conclusions concerning the transport properties of these alloys at low temperatures.

It is divided essentially into three parts:

- 1) a short review of the theory,
- 2) the experiments and the apparatus, and
- 3) the discussion of the results.



## PART 1

## THEORY

1.1 Historical Review

A discussion of the transport properties of metals, such as the electrical resistivity and the thermal conductivity generally involves the Boltzmann equation. The Boltzmann equation is a statistical approach to calculating the transport properties. There are detailed discussions of the Boltzmann equation in the literature (Ziman, Electrons and Phonons, Chapter 7) and only a brief review will be presented here.

For a steady state flow of electricity or heat by electrons in a metal there exists a distribution function,  $f$ , which represents the probability that the electron state designated by the wave vector  $\vec{k}$  will be occupied by an electron. This distribution function is dependent upon the velocity,  $\vec{v}$ , and the spatial coordinate,  $\vec{r}$ , of the electrons and is different from the distribution function in the absence of flow which we shall designate by  $f_0$ . We are primarily interested in the change with time of the distribution function due to three disturbing influences, 1) an electric field,  $\vec{E}$ , 2) a magnetic field,  $\vec{H}$ , and 3) a temperature gradient,  $\nabla T$ . The Boltzmann equation for this case is:

$$-e/n \left\{ \vec{E} + 1/c(\vec{v}_{\vec{k}} \cdot \vec{H}) \right\} \cdot \frac{\partial f}{\partial \vec{k}} - \vec{v}_{\vec{k}} \cdot \frac{\partial f}{\partial \vec{r}} + \frac{\partial f}{\partial t} \Big|_{\text{coll.}} = \frac{\partial f}{\partial t} \quad (1)$$



If the distribution function,  $f$ , returns exponentially to the equilibrium value,  $f_0$ , when the disturbing influences are removed then,  $\left. \frac{\partial f}{\partial t} \right|_{\text{coll.}} = -\frac{f - f_0}{\tau}$ , and a unique relaxation time,  $\tau$ , is said to exist and for a steady state,  $\frac{\partial f}{\partial t} = 0$ . Then, under these conditions the Boltzmann equation becomes:

$$-e/\hbar \left\{ \vec{E} + \frac{1}{c}(\vec{v}_k \cdot \vec{H}) \right\} \cdot \frac{\partial f}{\partial \vec{k}} - \vec{v}_k \cdot \frac{\partial f}{\partial \vec{r}} = \frac{f - f_0}{\tau} \quad (2)$$

In our experiments we have one and sometimes two of these disturbing influences equal to zero.

Wilson (The Theory of Metals, p. 197) by solving the Boltzmann equation has derived expressions for the electric conductivity,  $\sigma$ , and the thermal conductivity,  $K$ , for metals with cubic lattices:

$$\sigma = \frac{e^2}{12\pi^3} \int \frac{\tau v^2 ds}{\text{grad}_{\vec{k}} E} \quad (3)$$

$$K = \frac{k^2 T}{36\pi} \int \frac{\tau v^2 ds}{\text{grad}_{\vec{k}} E} \quad (4)$$

where the integration is over the area of the Fermi surface in momentum space.

The theory becomes much more complicated when a magnetic field is applied. In the free electron approximation the transverse electrical magnetoresistance vanishes (Ziman, p. 494). MacDonald and Sarginson (1952) have derived an expression for the transverse electrical magneto-





resistance assuming a non-isotropic and non-uniform electron gas. They assume a simple distribution of two equi-probable relaxation times,  $\tau_1$  and  $\tau_2$ . Their result is:

$$\frac{\Delta\rho}{\rho_{H=0}} = \frac{\tau_1\tau_2(\tau_1-\tau_2)^2 (e^2/m^2c^2)H^2}{(\tau_1+\tau_2)^2 + 4\tau_1^2\tau_2^2 (e^2/m^2c^2) H^2}$$

where  $\Delta\rho$  is the increase in the electrical resistivity above the resistivity  $\rho_{H=0}$  where  $H$  is the magnetic field strength. For low field  $4\tau_1^2\tau_2^2 (e^2/m^2c^2) H^2 \ll \tau_1^2 + \tau_2^2$  so that in this range there is a quadratic dependence of  $\Delta\rho/\rho$  on the magnetic field. Calculations based on an over-lapping, two-band model also produce an expression similar to this. Bethe (1931) suggested that the explanation of the magnetoresistance was in the deformation of the Fermi surface from the spherical shape. It then seems essential that any adequate theory must take into account the shape of the Fermi surface which is known to be quite distorted in many metals. Figure 2 shows the Fermi surface of copper as deduced by Pippard (1957).

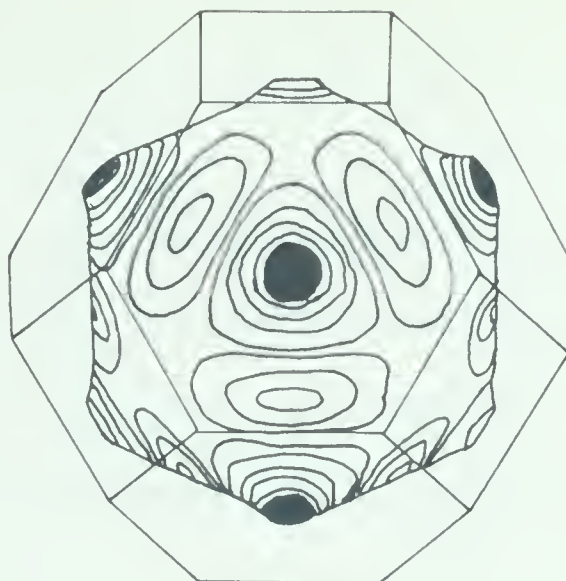
Ziman (1960, p. 504) assumes a non-spherical model of the Fermi surface and for polycrystalline specimens he finds the electrical magnetoresistance becomes:

$$\frac{\Delta\rho}{\rho_{H=0}} = B_t H^2 \sin^2 (\vec{J}, \vec{H}) + B_\ell H^2 \cos^2 (\vec{J}, \vec{H})$$

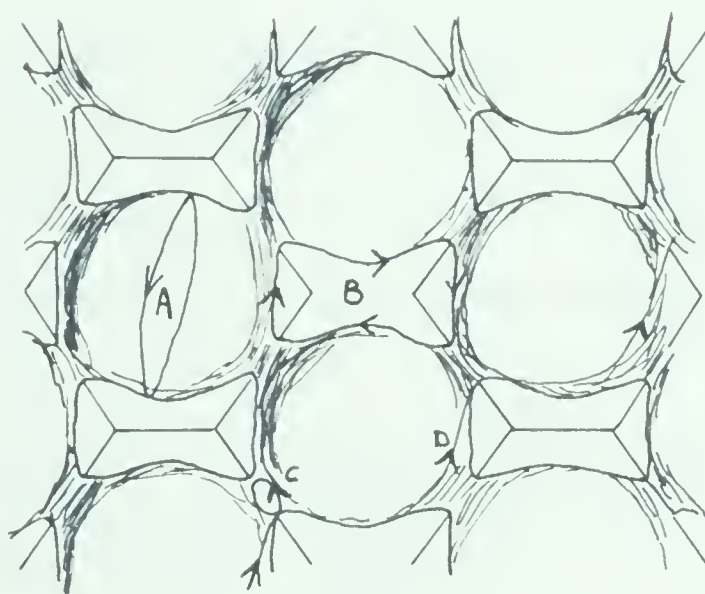
where  $\rho_{H=0}$  is the electrical resistance in zero magnetic field,  $B_t$  and  $B_\ell$  are scalar averages of the resistivity



Figure 2 . The Fermi Surface of Copper  
(Pippard, Morse ).



First Zone



Schematic:

- A. Belly orbit
- B. Dog-bone orbit
- C. Neck orbit
- D. Open path



tensor and  $\vec{J}$  is the electrical current. For a transverse field this reduces to:

$$\frac{\Delta\rho}{\rho_{H=0}} = B_t H^2$$

There is no difficulty now in understanding why the magnetoresistance arises and how the longitudinal and transverse magnetoresistance might be of the same order of magnitude since they are both determined by the anisotropy of the Fermi surface. Olsen and Rodriguez (1957) conclude that their observed magnetoresistance for copper is due to the anisotropy of the Fermi surface and that the Fermi surface probably touches the zone boundaries in the (111) directions as proposed by Pippard.

Assuming a two-band model in which part of the thermal conductivity,  $K_d$ , is due to a nearly full d-band and the remaining part,  $K_s$ , due to a nearly empty s-band, Kohler (1949) has shown that the thermal magnetoresistance is given by:

$$\frac{\Delta w}{w_0} = \frac{\left(\frac{1}{ecTL}\right)^2 \left(\frac{K_s}{N_s} + \frac{K_d}{N_d}\right) \left(\frac{K_s K_d}{(K_s + K_d)^2}\right) H^2}{1 + \left(\frac{1}{ecTL}\right)^2 \left(\frac{N_s - N_d}{N_s^2 N_d^2}\right) H^2}$$

where  $N_s$  and  $N_d$  are the number of electrons in the s and d bands respectively,  $T$  is the absolute temperature, and  $e$ ,  $c$ , and  $L$  are constants.





On the basis of lattice spacing studies Massalski and King (1960) have suggested that the distortion of the Fermi surface diminishes as the concentration of the solute is increased in the silver and copper alloys but increases in the gold based alloys. If this were true a vanishing magnetoresistance would be obtained as shown for the models discussed previously. However, gold based alloys also show negative magnetoresistance. Ziman (p. 350) mentions that he has considered a change in the Fermi surface also, but on this theory he obtains the wrong sign for the contribution to the thermoelectric power. He then suggests that the effect of alloying is simply to add electrons without giving rise to much change in the energy surfaces.

Korringa and Gerritsen (1953) gave a phenomenological theory in which they postulated an increase in the density of electron states in a region near the magnetic ion impurity. This increased density was suggested to lie close to the Fermi energy. The scattering of a conduction electron depends on the relative orientation of its spin and that of the magnetic ion. This spin dependence of the scattering explains the decrease of resistance in a magnetic field. The spins of the magnetic ions will be aligned by the field in which case the electron scattering is less than for randomly oriented ion spins. Their theory received



much support particularly by Yosida (1957) and Kasuya (1959) who suggest that the increase in the density of states is due to the resolution of the magnetic degeneracy of the ions. They suggest that this resolution is brought about by an exchange interaction between neighboring impurities and they use an effective molecular field as a model in their calculations.

The transport properties of this type of alloy are strongly influenced by the s-d interaction which is the interaction between the conduction electrons and the manganese ions. Yosida considers the perturbing potential due to this interaction to consist of two parts: 1) a spin dependent component and 2) a spin independent component. The spin dependent component is an exchange interaction and the spin independent component arises from an ordinary screened coulomb potential around the manganese ion. The results of Yosida for the electrical resistivity and the magnetoresistance of the copper-manganese alloys agree with experiment for the less dilute alloys (concentration of manganese greater than one per cent) but do not show the minimum and maximum in the electrical resistivity that is found for the very dilute alloys. A giant thermoelectric power is calculated by Kasuya using a model similar to Yosida's but he does suggest that some other mechanisms may also be contributing. The chief complications arise



from the degree of order of the impurity ions and from the complexity of the band structure of copper.

Bailyn (1961) has considered a spin dependent interaction also and has studied the anomalous transport properties of metals with magnetic ion impurities using a variational approach. To explain the minimum found in the resistivity he assumes a ferromagnetic model with an effective internal field to represent the interaction between the ions. The explanation of the minimum requires a transition toward an anti-ferromagnetic model as the temperature is lowered. Bailyn has done an approximate calculation of the depth of the minimum in the electrical resistivity which he measures by the quantity,  $\frac{\rho_4 - \rho_{20}}{\rho_{20}}$ , where  $\rho_{20}$  is the resistivity at 20°K. He finds that the depth of the minimum is 23 per cent when he assumes that the ferromagnetic and anti-ferromagnetic fields used in the models are equal in strength.

The existence of the ferromagnetic and anti-ferromagnetic transition and the validity of the molecular field model for the copper-iron alloys has yet to be established (Bailyn (1960)).





## 1.2 The Electrical Resistivity

According to Matthiessen's rule the electrical resistivity of a metal may be written in the form  $\rho(T) = \rho_0 + \rho_i(T)$  where  $\rho_0$  is the residual resistivity and  $\rho_i(T)$  is the ideal resistivity. The residual resistivity is independent of the temperature but is dependent on the type and concentration of the impurities present in the metal. Bloch (1930) has derived the temperature dependence of  $\rho_i(T)$  to be  $\rho_i(T) = 4(T/\theta)^5 J_5(\theta/T) \rho_\theta$  for a free electron metal. At low temperature  $J_5 = \text{constant}$  and  $\rho_i(T) \simeq 500 (T/\theta)^5 \rho_\theta = cT^5$ . Ziman (p. 365) gives a qualitative appreciation of the  $T^5$  rise of  $\rho_i(T)$  above  $\rho_0$  and states, "This is as characteristic a quantum effect as the  $T^3$  law of specific heats".

For the behavior of alloys with magnetic ion impurities a rise in the resistance above the value  $\rho_0$  is found as the temperature is lowered as shown by the curve CD of Figure 1. Empirically, the electrical resistance can now be written:

$$\rho(T) = \rho_0 + \rho_i(T) + \rho_a(T)$$

where  $\rho_a(T)$  is the anomalous increase in the resistivity. Pearson (1955) finds empirically that the temperature and concentration dependence of  $\rho_i(T)$  can be represented  $\rho_a = f(r_c)(T_{\min} - T)^n$  between  $T_{\min}$ , the temperature of the minimum in the resistivity, and 4.2 °K where  $n \simeq 2$  and



where  $f(r_c)$  is a constant for a particular alloy and appears to be a linear function of  $\rho_0$ . The temperature  $T_{\min}$  is dependent on the concentration.

### 1.3 The Electron Thermal Conductivity

We have assumed that the electron conductivity is additive in a first approximation to the lattice thermal conductivity,  $k_g$ , so that we may write  $k = k_e + k_g$ .

The electron thermal conductivity,  $k_e$ , is limited by two resistive processes. We may write  $1/k_e = w_0 + w_i$  where  $w_0$  is due to the scattering of electrons by impurities and at low temperatures is a much larger resistivity than  $w_i$  which is due to the scattering by phonons. The temperature dependence that is deduced experimentally by White (1953) for pure copper is  $w_i = 7.1 \cdot 10^{-6} T^{2.4}$  cm deg./watt. The theoretical expression derived for a free electron metal is  $w_i = c T^2$ . The value of  $w_0$  is related to the residual resistivity  $\rho_0$  by the Lorenz relation  $L_0 = \frac{\rho_0}{w_0 T}$ . Adopting the experimental value for  $w_i$  we can then write for the electron thermal resistivity  $1/k_e = A/T + 7.1 \cdot 10^{-6} T^{2.4}$  where  $A = \rho_0/L_0 = w_0 T$ . At low temperatures ( $T < 10^\circ\text{K}$ )  $w_i$  is much less than  $w_0$ . Since  $\rho = \rho_0 + \rho_a$  at temperatures lower than  $T_{\min}$  it was of interest to try to detect an effect in the thermal resistivity due to the scattering of the electrons by the iron impurity.



#### 1.4 The Lattice Thermal Conductivity

The lattice conductivity is a measure of the heat carried by the phonons and the scattering processes limiting the lattice conductivity are described by the following equation:

$$1/k_g = W_E + W_B + W_D + W_U.$$

The thermal resistivity,  $W_E$ , is due to the scattering of phonons by the conduction electrons and the thermal resistivity,  $W_D$ , is due to the scattering of phonons by dislocations. Both  $W_E$  and  $W_D$  vary inversely as the square of the absolute temperature. The thermal resistivity components  $W_B$  and  $W_U$  are due to the scattering of phonons by point defects and by phonons respectively. These latter two components dominate the behavior of  $k_g$  at liquid oxygen temperatures. At low temperatures ( $T < 10^\circ\text{K}$ ) we may then write:  $1/k_g = W_E + W_D = DT^{-2}$  Klemens (1954) has shown that in the absence of dislocations the lattice resistivity,  $W_E$ , can be related to the ideal electrical resistivity. At low temperatures the lattice resistivity becomes  $W_E = \frac{1}{313} w_i(T) \left(\frac{\theta}{T}\right)^4 N_a^{4/3}$  where  $w_i$  is the ideal electron thermal resistivity and  $N_a$  is the number of conduction electron per atom. For copper using the experimental values for  $w_i$  and putting  $\theta = 315^\circ\text{K}$  he obtained  $W_E = 710 \text{ } \tilde{T}^2$ .





## PART 2

## THE EXPERIMENTAL WORK

2.1 General

The low temperature cryostat used for these experiments is shown in Figure 3, and has been described first in the literature and recently more thoroughly by Adler (1960). With this cryostat the measurement of electrical and thermal conductivity can be made on the same sample over the temperature range from 2 °K to 150 °K.

The specimen is mounted onto a pillar that is thermally anchored to an inner helium chamber. The temperature of the chamber can be regulated below 4.2 °K by maintaining a constant pressure over the helium boiling in it and at temperatures above 4.2 °K by using an electronic temperature controller to heat the empty chamber. The pressure and therefore the temperature of the boiling helium is controlled accurately by means of a cartesian manostat (Gilmont (1950)). The electronic temperature controller (Dauphinee and Woods (1955)) maintains the temperature of the inner chamber constant to within 0.001 °K. Essentially the system consists of a thermocouple soldered to the top plate of the inner helium chamber with a reference junction at the ambient temperature of the liquid helium in the dewar. The d.c. potential of this couple is then compared to the voltage drop across a resistor through which a constant



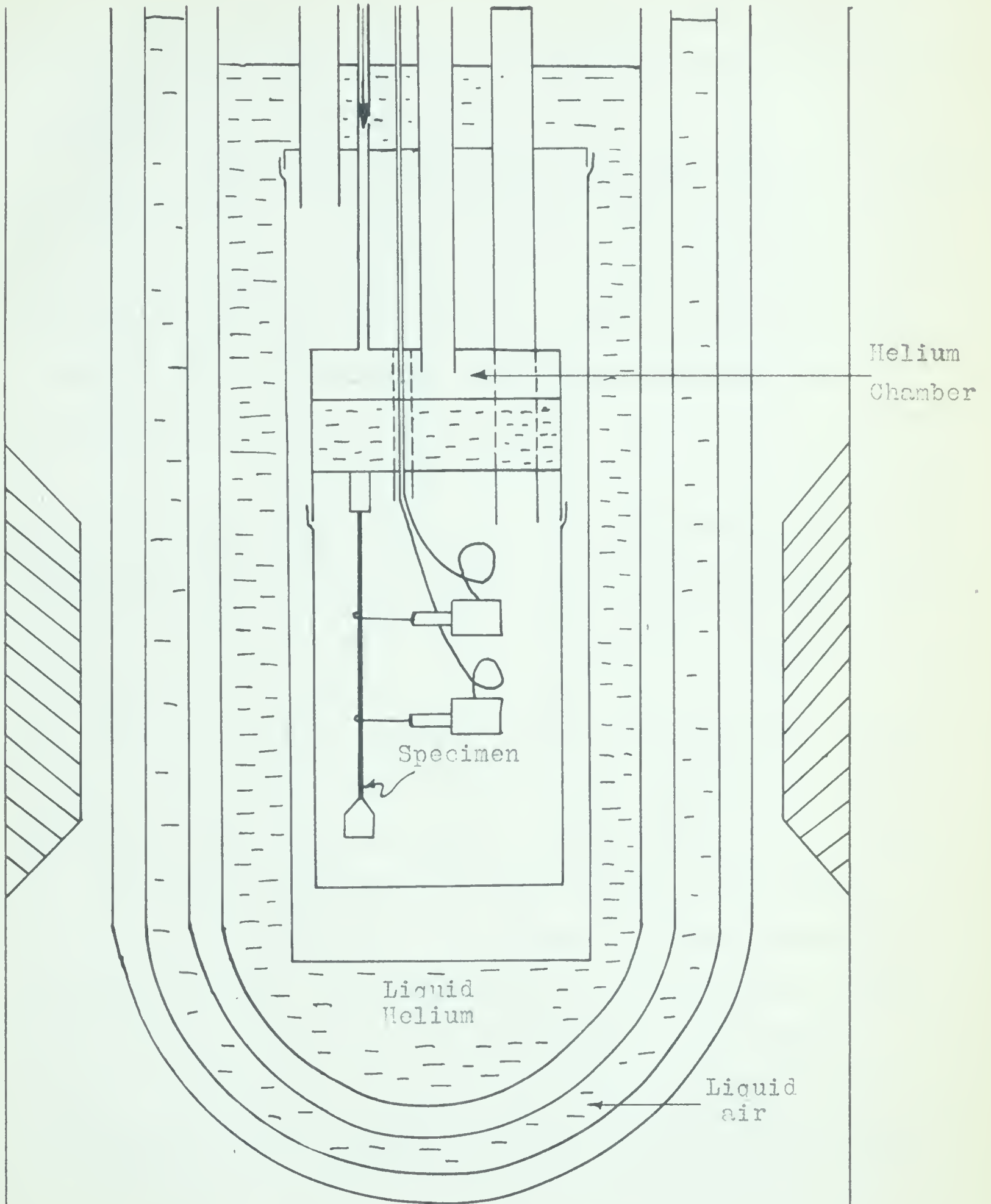


Figure 3 . The Cryostat in the Magnet



current is flowing and the difference voltage is amplified by a chopper amplifier with a gain of  $10^7$ . The amplifier output regulates the current in a heater mounted on the top of the inner helium chamber.

Temperature measurements were made with two identical gas thermometers attached to the specimen. Use of a differential manometer system allows measurement of temperature differences that are only a few percent of the mean sample temperature with one percent accuracy. The electrical resistivity,  $\rho$ , is determined using

$$R = V/I = \rho(\ell/A)$$

where  $R$  is the resistance of the specimen. The potential difference,  $V$ , is measured using the galvanometer amplifier and the current,  $I$ , is measured using a precision ammeter. The shape factor,  $\ell/A$ , is the ratio of the length,  $\ell$ , of the specimen between specimen leads to the cross-sectional area,  $A$ , of the specimen. The relative accuracy of measurements on a particular specimen is about one percent. With the relatively short thick specimens with which thermal conductivity measurements can be made a larger uncertainty usually arises in the determination of the absolute values of the resistivity due to the uncertainty in the shape factor. However the shape factor does not enter in the determination of the Lorenz ratio or the magnetoresistance provided that, for the Lorenz ratio, the electrical and thermal measurements are made on the same specimen.





The electrical resistance of the specimen was first measured at 4, 80, and 295 K using potential leads of very fine (0.0045 ") copper wire and a dipstick arrangement described by Rogers (1962). The shape factor for these measurements was calculated from the accurately measured values of the length and area. When good thermal connections were made to the specimen for measurements in the cryostat the distance to measure between contacts was uncertain because of their greater area. Instead the electrical resistance measured in the cryostat was compared with the earlier measurements to obtain the new shape factor. The uncertainty in the determination of the new shape factor was about 1.5 per cent.



## 2.2 The Gas Thermometers

The gas thermometers used for the differential thermometry and for the determination of the absolute temperature are described in detail by Rogers (1962). They are shown schematically in Figure 4 and only the pertinent details will be discussed here.

The upper (cold) thermometer is operated at constant volume and its temperature is given by:

$$T/P = T_o/P_o \left\{ \frac{1 + \Delta}{1 + \Delta_o} \right\} + \alpha,$$

where  $T_o$  is the filling temperature,

$P_o$  is the filling pressure,

$v$  is the volume at temperature  $t$ ,

$V$  is the volume of the bulb at temperature  $T$ ,

$$\Delta = \frac{vT}{Vt}, \quad \Delta_o = \frac{vT}{Vt} o, \quad ,$$

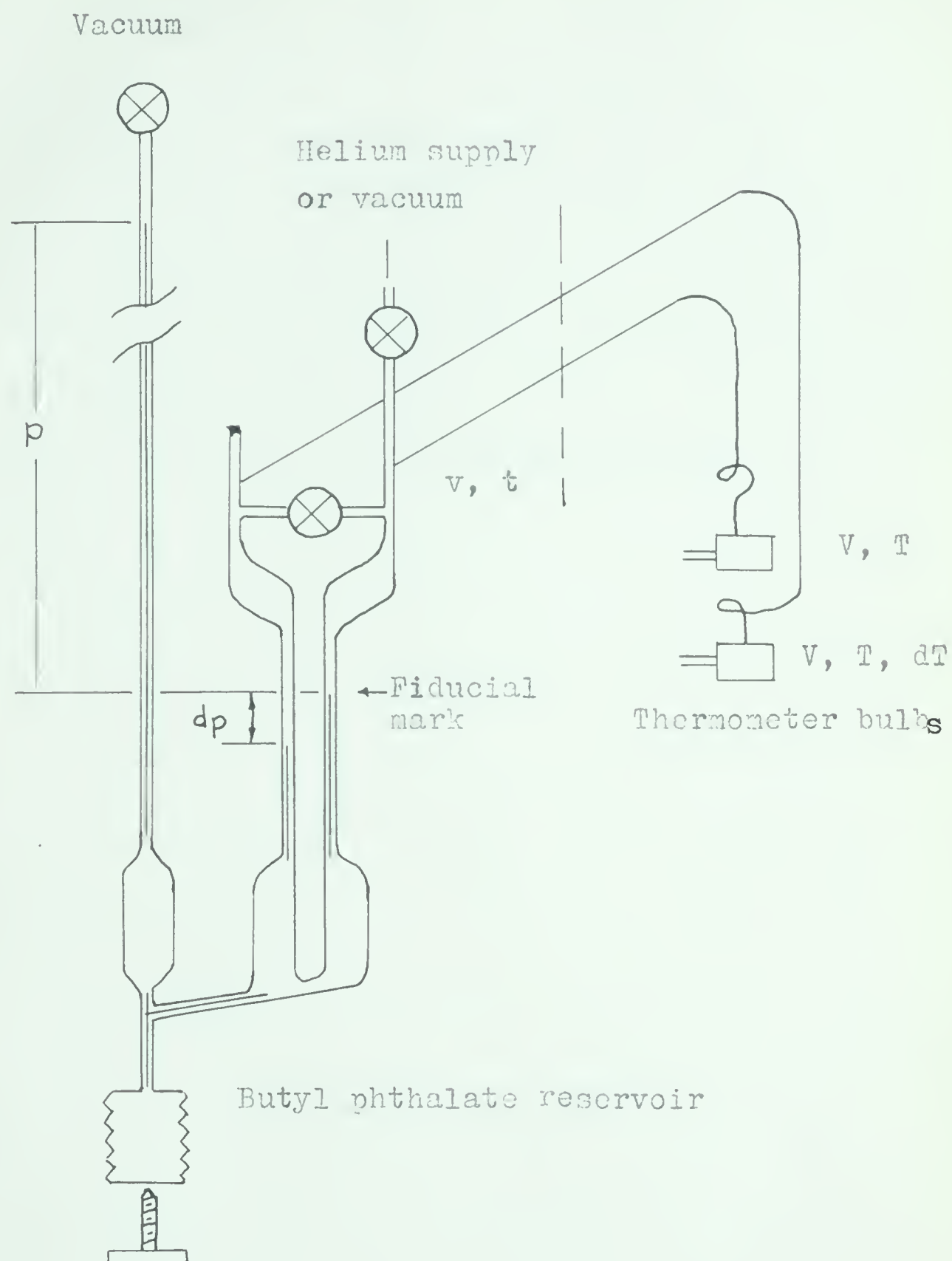
and  $\alpha$  is a small virial correction which is constant when  $T$  is greater than 5 °K.

The temperature variation of  $\frac{1 + \Delta}{1 + \Delta_o}$  is shown in Figure 5 as a function of temperature for two different filling temperatures.  $\frac{1 + \Delta}{1 + \Delta_o}$  is approximately equal to one and is the correction for the small amount of gas that is not at the temperature of the thermometer bulbs.  $\alpha$  is a correction arising from the departure of helium gas from ideal behavior. In differential thermometry the temperature difference,  $\delta T$ , between the two thermometers is:

$$\delta T/\delta P = \left\{ T_o/P_o \right\} \left\{ \frac{(1 + \Delta)^2}{1 + \Delta_o} + \frac{AT^2}{vt} \right\},$$



Figure 4. The Gas Thermometers (Rogers 1962)







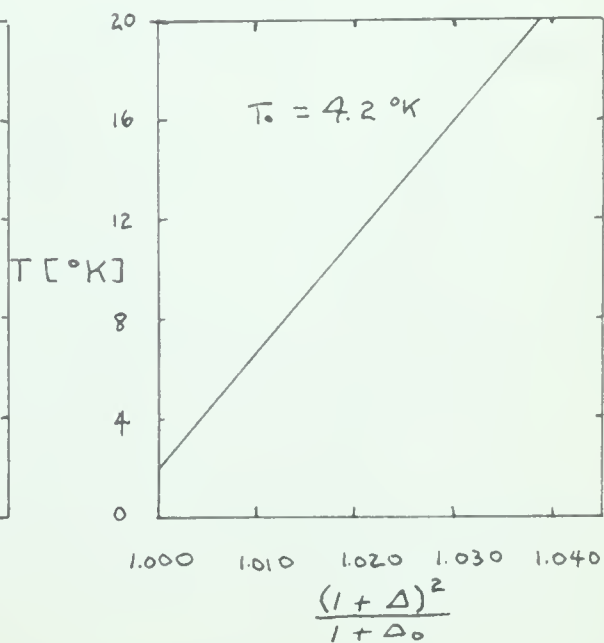
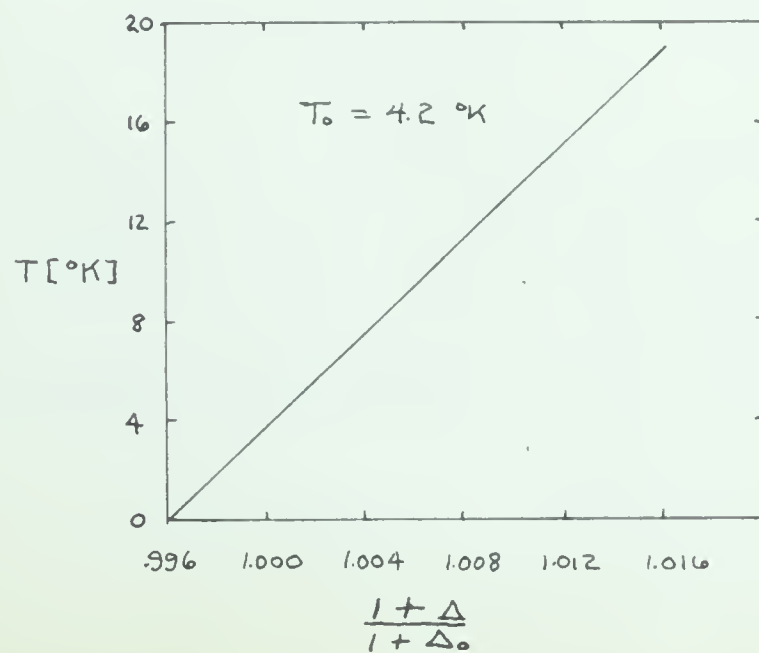
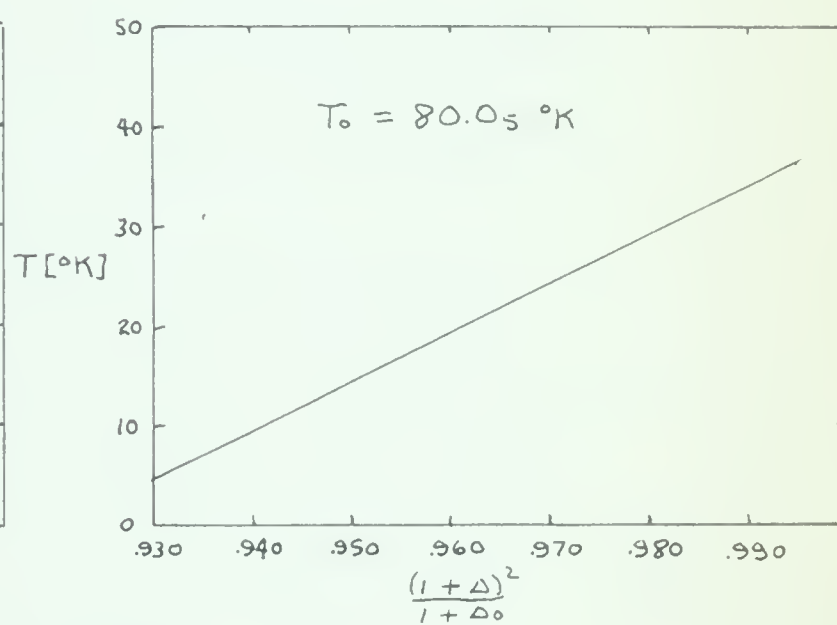
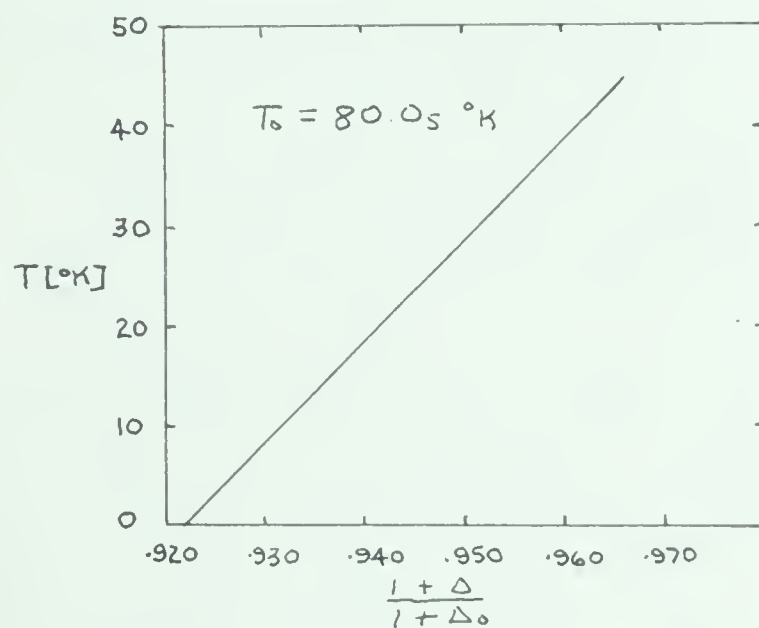
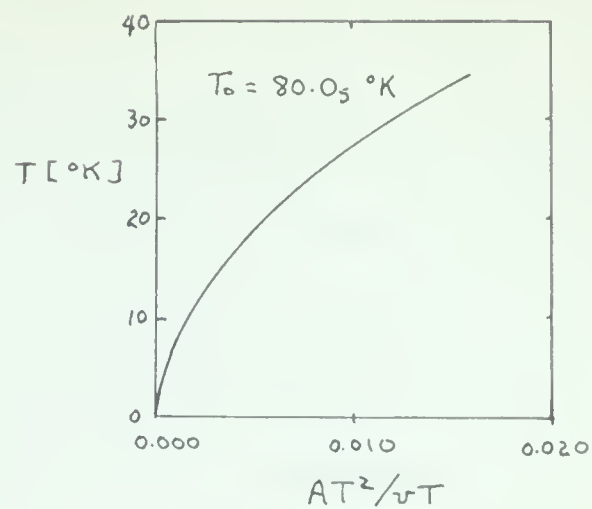
where  $A$  is the area of the precision glass capillary. This formula can be derived from the ideal gas law (Rogers (1962)). Graphs of  $\frac{(1 + \Delta)^2}{1 + \Delta_0}$  and  $\frac{AT^2}{vt}$  as a function of temperature are shown in Figure 5. The thermometers were replaced at the beginning of this work and were calibrated. For the temperature range between 2 and 4 °K the temperature measured using the gas thermometers agreed within a few thousandths of a degree with the temperature determinations from the vapour pressure of the helium boiling in the inner chamber (using the 1958 He<sup>4</sup> vapour pressure scale.).



## Figure 5. Gas Thermometer Corrections

$$V = 4.457 \text{ cm}^3$$

$$v = 1.395 \text{ cm}^3$$





### 2.3 The Galvanometer Amplifier

Potential differences were measured on a galvanometer amplifier built by Rogers (1962). This is a negative feedback amplifier built from a design by MacDonald (1947). Fenton (1962) has given a short description of the device also that is based on the arguments of MacDonald.

The potential difference across the specimen is given by

$$E = IR_f = 2cdR_f$$

where  $2d$  is the deflection of the secondary galvanometer when the current,  $I$ , is reversed through the specimen,

$R_f$  is the feedback resistance

and  $c$  is a parameter of the galvanometer system.

Both Rogers and Fenton have shown that  $c$  is almost constant but has a weak dependence on the sum  $R_1$  of the primary galvanometer and lead resistances, the current gain  $\alpha$ , and the feedback resistor  $R_f$ . They obtain

$$c = E/2d R_f = 1/\beta (1 + R_1/\alpha R_f)$$

where  $\beta$  is the deflection sensitivity of the secondary galvanometer and for our instrument was 3750 mm./micro-amp. The current gain  $\alpha$  is defined by  $\alpha = I/i$  where  $I$  is the current through the secondary galvanometer and  $i$  is that through the primary.





In practice the current gain may vary during the course of an experiment so the galvanometer amplifier was calibrated at the start and finish of each experiment with a Cambridge vernier potentiometer. The value of  $c$  rises as  $R_f$  is decreased and is 1.6 per cent higher when  $R_f = 10$  ohms than when it is 100 ohms at which feedback the calibrations were done. Values of  $R_f$  lower than 10 ohms were never used.



## 2.4 Specimen Preparation

### a) Preliminary

The copper used in the preparation of the alloys was stock rod available in the Physics Department in the form of one inch diameter rods having a nominal purity of 99.9 percent. It was originally supplied by Noranda Copper and Brass, Ltd. The predominant impurities were quoted to be iron, silver and zinc. The iron added in the preparation of the alloys was electrolytic dust having a nominal purity of 95.4 percent.

The ratio of the residual resistivity to the resistivity at room temperature is a sensitive test of purity of a metal specimen. The value of this ratio for a pure, annealed specimen of the copper was  $9 \times 10^{-3}$ . This value compares reasonably well with the value ( $6 \times 10^{-3}$ ) for the copper used by Gerritsen (1953) in making his copper-manganese alloys. It is possible however that some of the impurities were present in the form of oxides which segregate at the grain boundaries and therefore have a much smaller effect on the residual resistivity than unoxidized impurities.

A master alloy containing four percent of iron was prepared using the induction furnace in the Department of Mining and Metallurgy. Since it is impossible to levitate copper and iron they were melted in a recrystallized alumina crucible made by Morgan Refractories, England. Melting the alloys in the induction furnace ensured that the components



mixed thoroughly although iron at this concentration in copper does not make a homogeneous alloy. This sample was prepared under an argon atmosphere. Cracks appeared in the crucible and only by limiting the power was the copper prevented from vaporizing. The alloy was allowed to solidify in the crucible and dendrites such as those shown in Figure 6 were observed. The cooling time to room temperature was approximately twenty minutes.

#### b) Preparation of the Alloys

An alloy containing 0.5 percent of iron was prepared in the resistance-wound furnace by melting part of the master alloy with some copper. This alloy was prepared in a quartz boat in a vacuum where the pressure was lower than  $5 \times 10^{-4}$  mm. of Hg. Some homogenation of the melt was achieved by vibration originating from the mechanical pump and later the alloy was severely cold worked at room temperature when its diameter was reduced by fifty percent or more. Since the mixing was poor a vertical concentration gradient was expected and was found on microscopic examination of this alloy.

Further alloys were then prepared by placing pieces of this 0.5 percent alloy and of pure copper in a quartz boat and melting them in a vacuum. The temperature was held above  $1200^{\circ}\text{C}$  for periods longer than 1/2 hour in order that mixing by diffusion could also take place. The





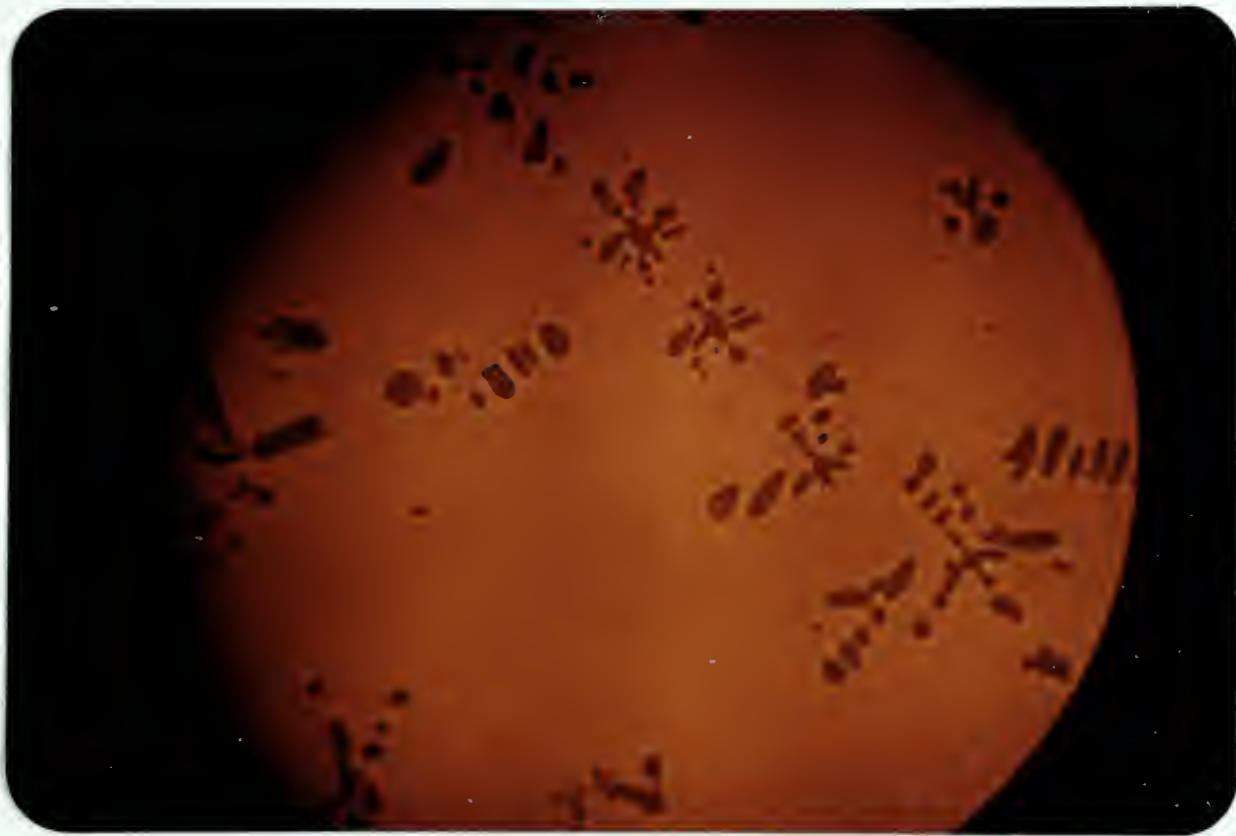


Figure 6. Dendrites in 4 percent Copper-iron alloy. The diameter of this alloy is about 0.6 mm.



weight of each sample before and after melting showed that the loss of copper due to vaporization was negligible. The vacuum above the melt each time was  $5 \times 10^{-4}$  mm. of Hg. Melting in high vacuum minimizes losses of iron into oxides at the surface and the importance of this and other losses is discussed under specimen purity. The sample was cooled by forcing compressed air between the sample tube and the inner wall of the furnace.

#### c) Drawing and Annealing

The freshly cooled ingots were 6 or 7 centimeters in length with a diameter of 1 centimeter. They were cold worked in a roller until their diameters were less than 5 millimeters and then they were annealed for two hours. An annealing temperature of  $700^{\circ}\text{C}$  was chosen since the equilibrium solid solubility of iron in copper decreases rapidly with increasing temperature. It is approximately 0.2 percent at  $700^{\circ}\text{C}$ . After this initial annealing each sample was drawn through dies to the appropriate diameter for the experiments and then short lengths at each end were machined to a diameter of 0.040 inches. Finally they were again annealed at  $700^{\circ}\text{C}$  for two hours and mounted in the cryostat.

#### d) Specimen Purity

Many authors have found that such effects as differences in vapour pressure of the components of alloys



and surface oxide layers cause large discrepancies between the composition by weight determined before melting and the composition of the resulting ingot. However, the concentration of dilute alloys can be determined from measurements of the resistivity at 4 °K.

The resistivity increase per atomic percent is independent of concentration for small amounts of impurity (Pearson 1955). For solute concentrations,  $c$ , less than 0.2% we write:

$$\rho_{\text{alloy}} \text{ 4}^{\circ}\text{K} = \rho_{\text{pure}} + \alpha c \approx \alpha c$$

The value of  $\alpha$  is 11.0 ohm-cm./atomic percent and thus a measurement of  $\rho_{4^{\circ}\text{K}}$  gives a measure of the amount of iron in solid solution. The solute concentrations determined by weight for each of the alloys were about fifty percent higher than the values determined using the resistivity at 4 °K.

#### e) Specimen Mounting

Annealed copper wires 0.025 inches in diameter connect the thermometer bulbs to the specimen. The connections to the thermometers contain a section that is a good thermal link but an electrical insulator. The potential leads that connect to the galvanometer amplifier are soldered to the 0.025 inch wire as shown in Figure 8. The electrical leads are thermally anchored to the copper pillar to prevent heat conduction to the specimen from the room temperature





region; also the thermometer bulbs and the specimen chamber are gold plated to reduce transfer of heat by radiation.

The leads to the specimen were soldered with an eutectic alloy of bismuth and cadmium which has a melting point of  $140^{\circ}\text{C}$ . This solder does not become superconducting above  $0.8^{\circ}\text{K}$ . Other solder joints were made with Woods' Metal or soft solder.



## 2.5 The Resistance-Wound Furnace

A small furnace with two heater windings was built for melting and annealing the alloys. The main coil, made of Kanthal heating wire, was wound on a grooved porcelain tube with a 1.2 inch diameter bore. The auxiliary winding was 60% platinum 40% rhodium alloy wire wound on a 2.1 inch diameter porcelain ring that was protected on the outside by two stainless steel heat shields. The whole furnace was mounted on a transite base. The auxiliary winding produces a hot zone about 13 centimeters from one end. Two curves of the temperature distribution along this furnace are shown in Figure 9. A diffusion pump was built onto the oven rack in order that the specimen preparation could be done in vacuum.

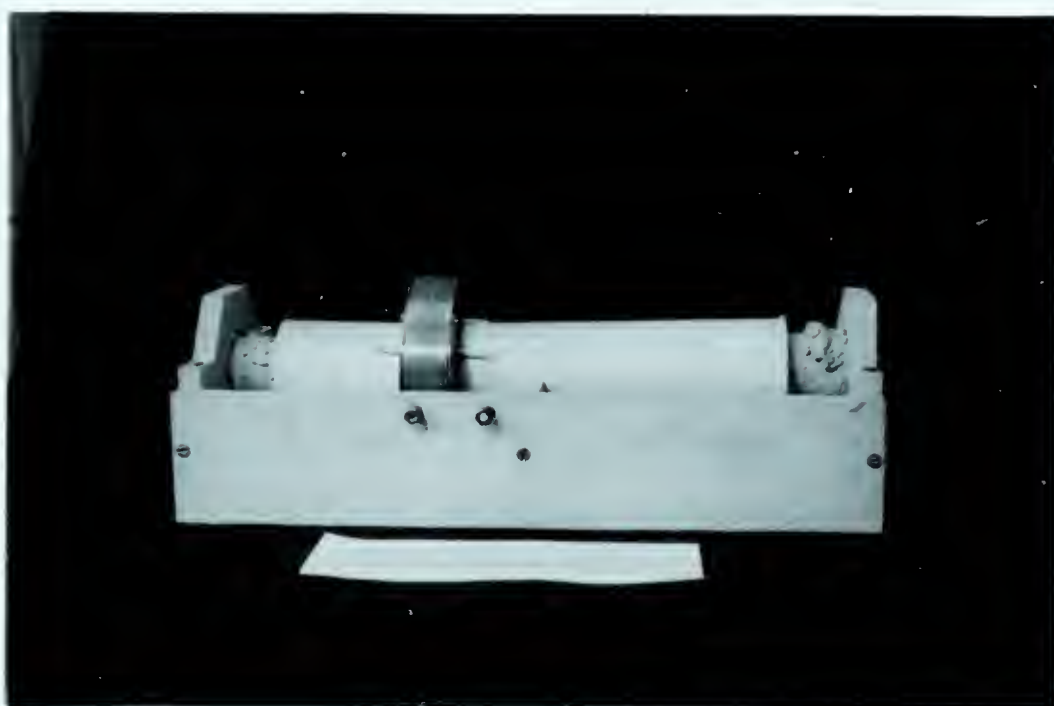
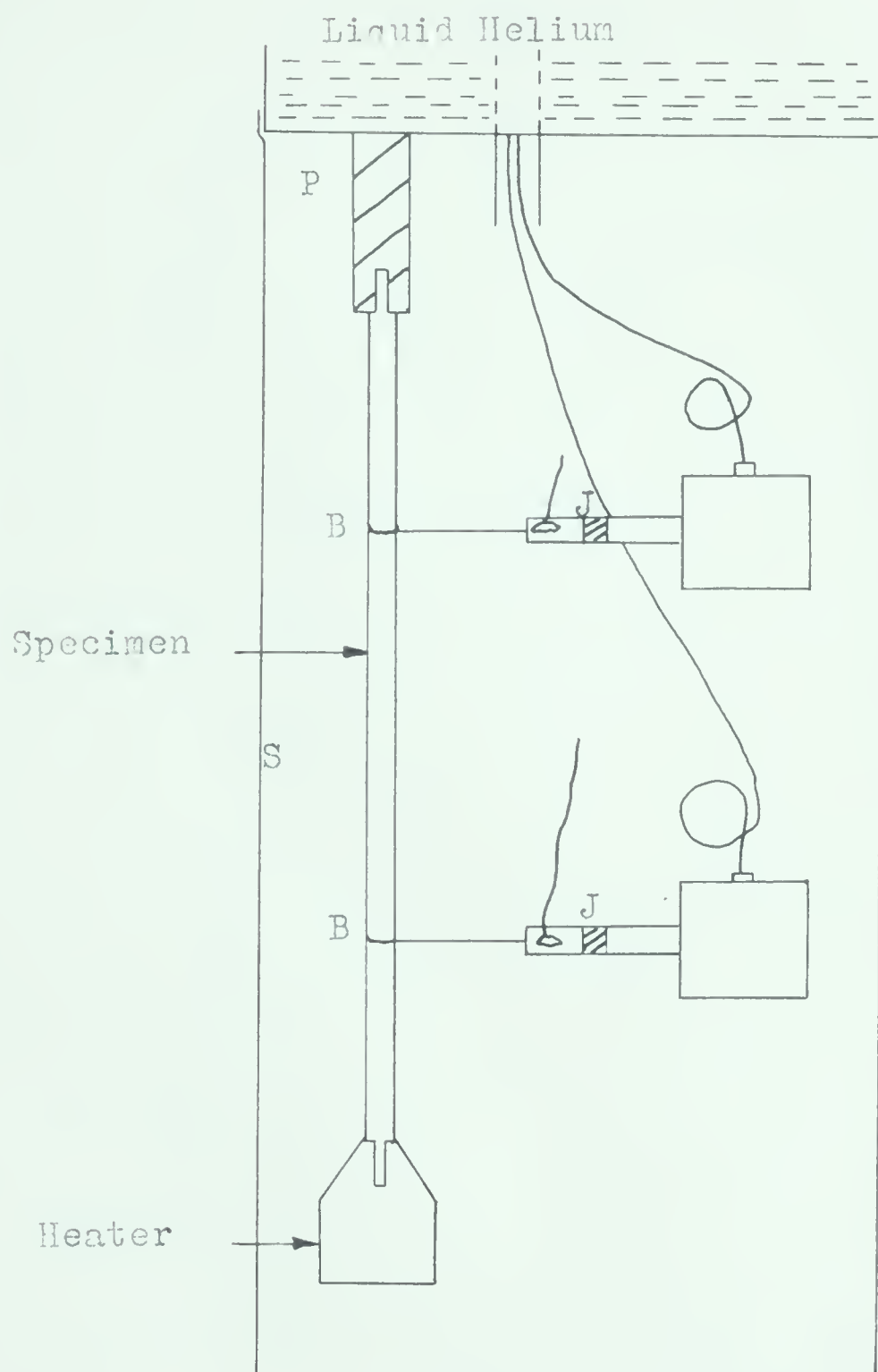


Figure 7. The Resistance-wound Furnace



Figure 8. Specimen Chamber



P - Copper Pillar

J - Thermally conducting, electrically insulating junction

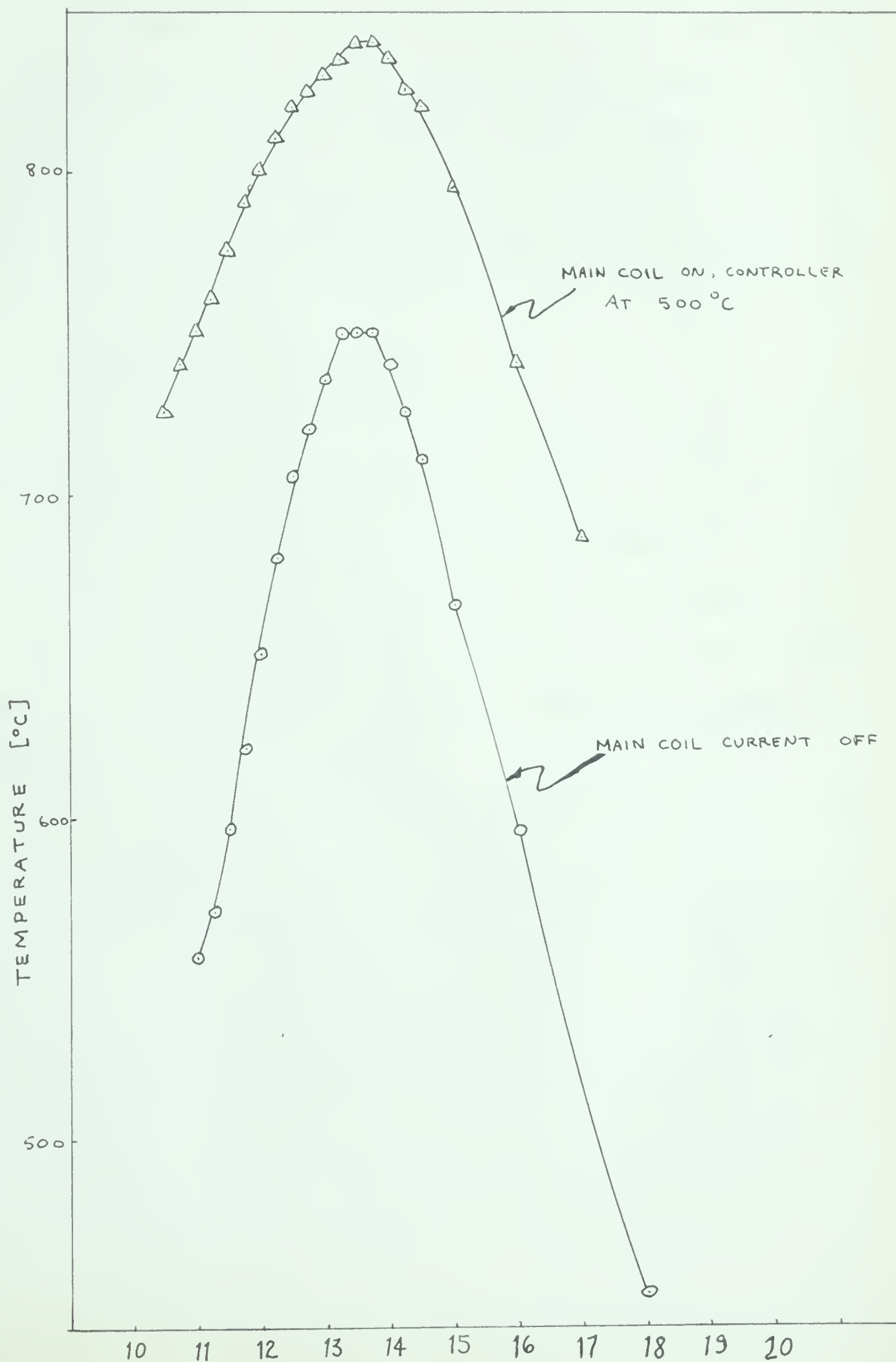
B - Bi-Cd solder, sample to 0.025" leads

S - Gold plated radiation shield





Figure 9 . Temperature Distribution Curves of Furnace  
( auxiliary current at 10.4 amperes)





## 2.6 The Magnetic Field

For the magnetoresistance measurements the cryostat and controller were moved to the large magnet in the Low Temperature Laboratory. The maximum possible pole separation was used into which the outer dewar fitted with less than 1/2 inch to spare. Some curves were drawn to show the field strength at the approximate position of the sample and are shown in Figure 10.

## 2.7 Experimental Procedure

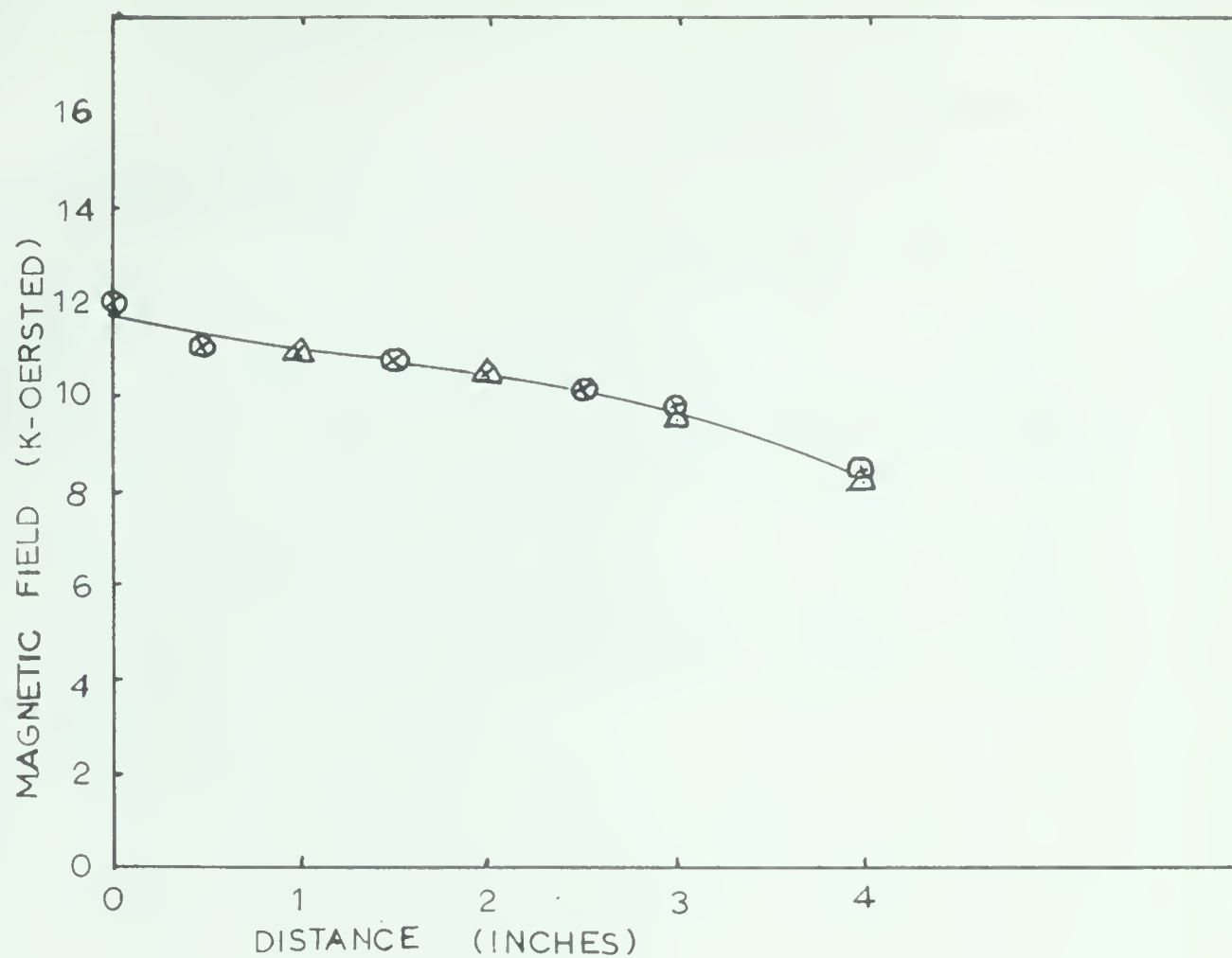
The specimen was mounted in the cryostat and its room temperature resistance was measured. The shape factor was calculated by comparison with the resistivity of the same sample obtained using the dip-stick arrangement. The cryostat was then cooled with liquid air at which temperature the thermometers were filled and the resistance of the specimen was again measured.

The dewar arrangement was then changed to that shown in Figure 3. Measurements were made in the 4 to 30 °K range using the electronic temperature controller to regulate the temperature. The thermometers were then filled to a higher pressure at the ambient boiling point of helium and measurements were taken in the 2 to 8 °K range.

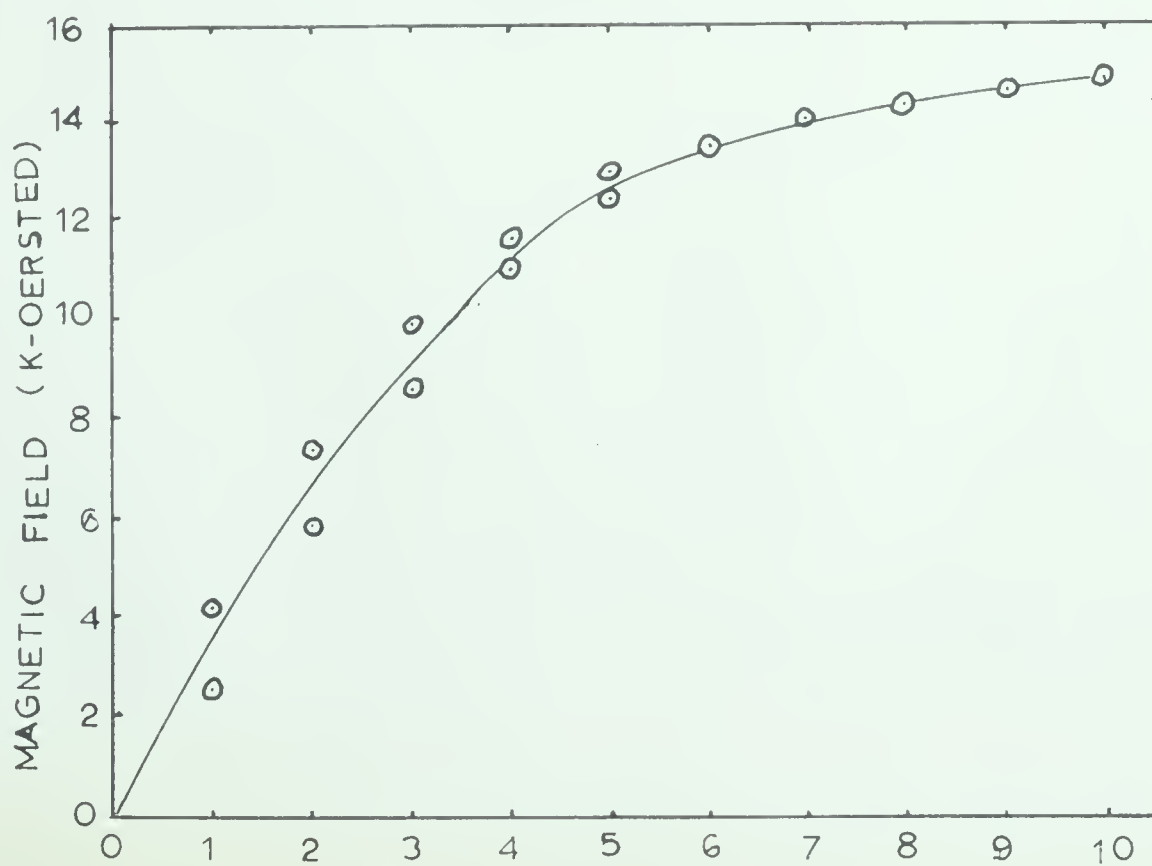


Figure 10. The Magnetic Field

- 1) measurements radially outward from the center of the field



- 2) measurements at the center as a function of the regulator current





## PART 3

3.1 Experimental Results

The values for the electron thermal conductivity were calculated using

$$k_e = (A/T + 7.1 \times 10^{-6} T^{2.4})^{-1}$$

where  $A = \rho_0/L = 1/(k_0/T)$  and  $L$  is the Lorenz number.

Plotting  $k/T$  versus  $T$  for the measurements below 5 °K will yield the value of  $k_0/T$  by extrapolation to 0 °K. The

lattice thermal conductivity,  $k_g$ , is obtained by subtracting the electron thermal conductivity from the total thermal conductivity.





Figure 11. Electrical Resistance of Pure Copper and Alloys

Values for 0.0043% and 0.056% are from White and Woods (1935)

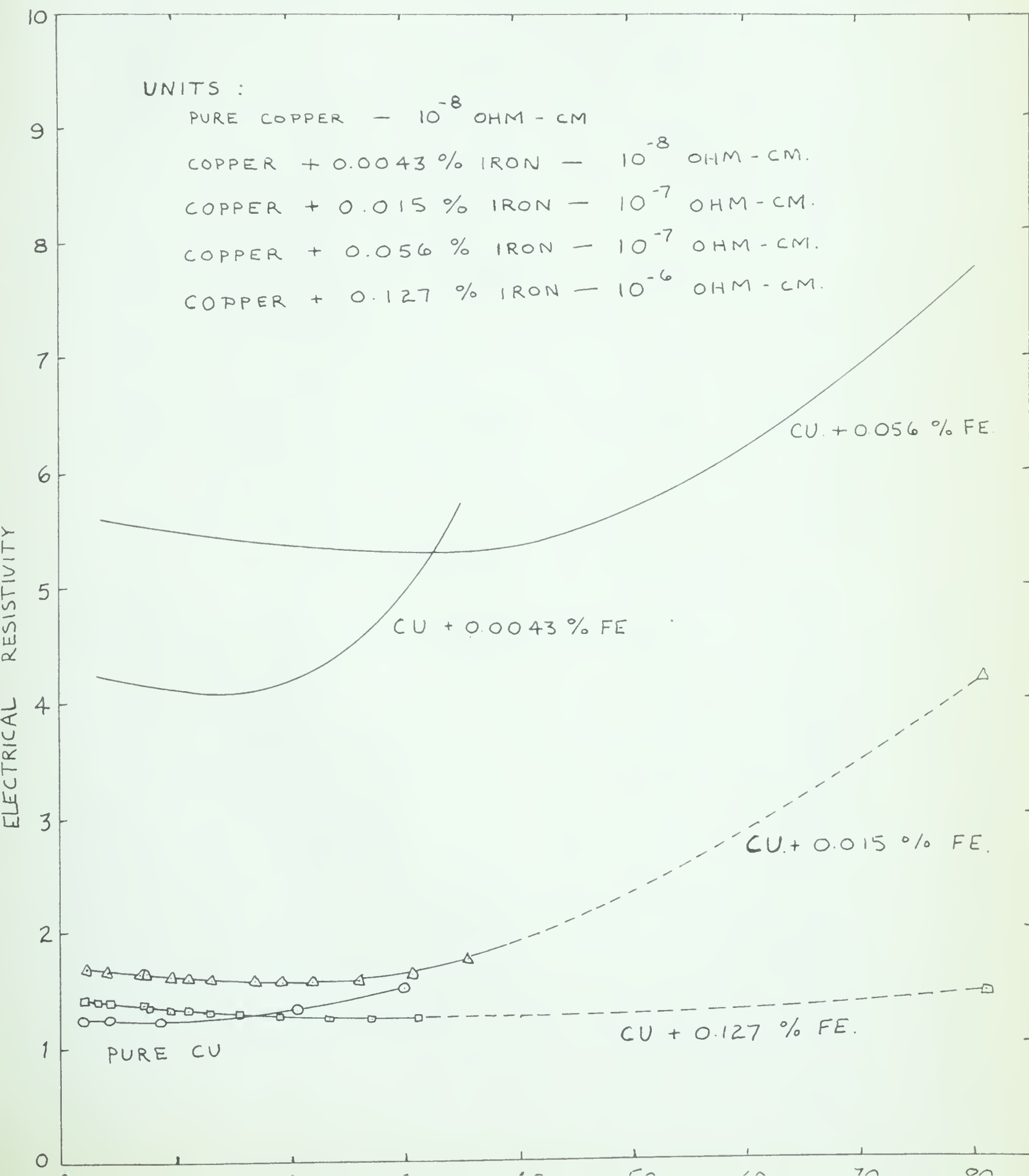




TABLE 1  
Copper + 0.015% Iron

T °K	k W/cm.°K	k <sub>e</sub> W/cm.°K	k <sub>g</sub> W/cm.°K	ρ 10 <sup>-7</sup> ohm-cm.
1.52				1.72
2.00*	0.325	0.310	0.015	
2.03	0.328			1.71
2.35	0.382			1.69
2.73	0.441			1.68
3.21	0.533			1.68
3.66	0.614			1.67
4.00*	0.680	0.627	0.053	
4.23	0.692			1.67
5.36	0.854			1.67
5.55	0.952			1.67
6.00*	1.04	0.930	0.115	
6.46	1.13			1.65
7.32	1.19			1.64
7.71	1.25			1.64
8.00*	1.42	1.24	0.18	
9.43	1.75			1.62
10.00*	1.84	1.57	0.27	
11.23	2.11			1.60
12.88	2.43			1.59
14.81	2.79			1.58
15.00*	2.79	2.30	0.49	
16.85	3.16			1.57
19.28	3.64			1.56
20.00*	3.69	3.06	0.63	
22.00	3.92			1.56
25.00*	4.30	3.60	0.70	
25.97	4.40			1.57
30.00*	4.76	4.20	0.56	
30.55	4.84			1.62
35.58				1.75

\* = smoothed value from graph



Figure 12. Thermal conductivity of Neon + 0.015% Iron Alloy

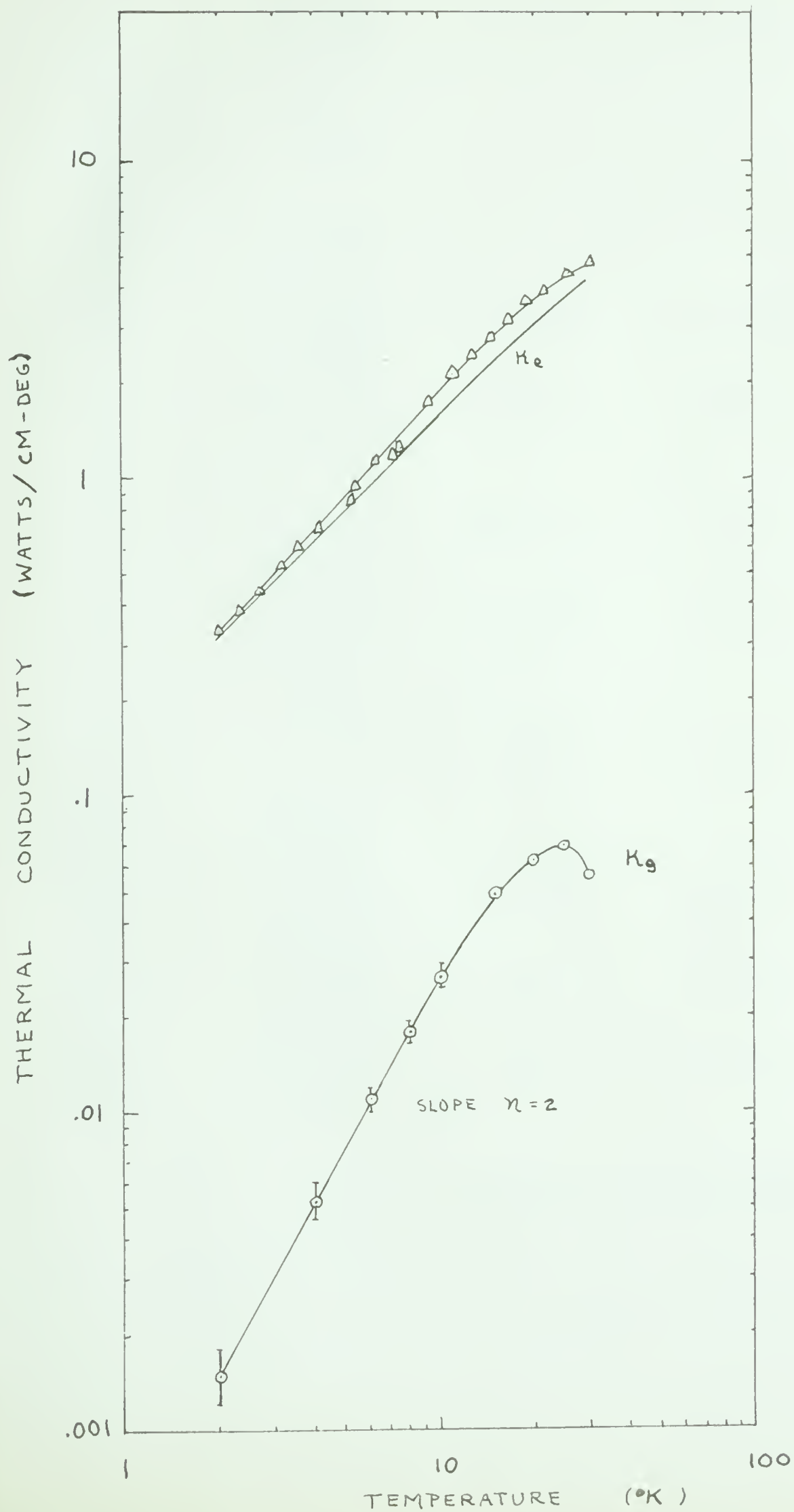






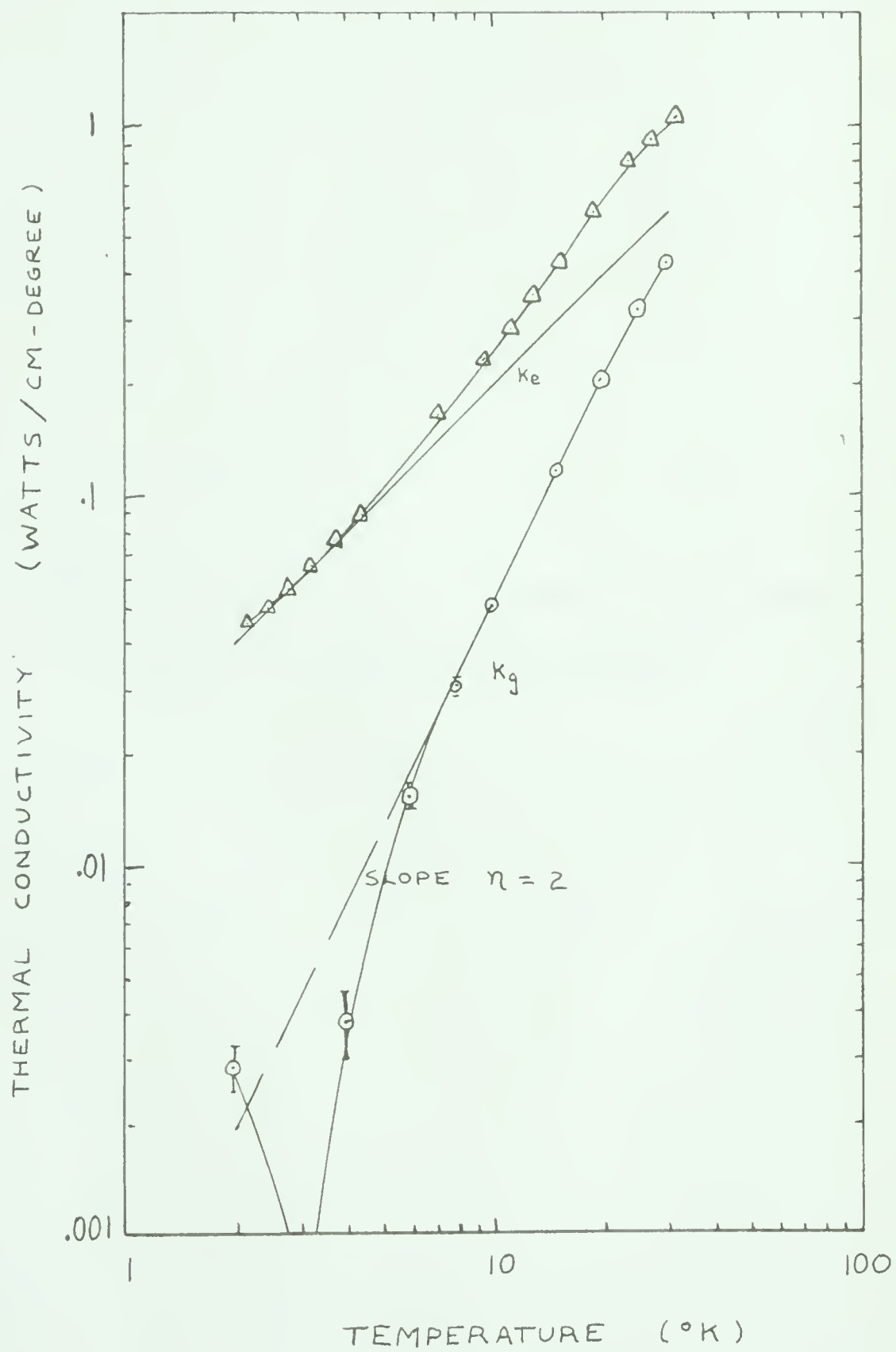
TABLE 2  
Copper + 0.127% Iron

T °K	k W/cm.°K	k W/cm.°K	k <sub>g</sub> W/cm.°K	$\rho$ 10 <sup>-6</sup> Ω cm.
2.00	0.0420*	0.0392	0.0028	
2.18	0.0445			1.42
2.46	0.0484			
2.80	0.0551			
3.00				
3.26	0.0639			1.41
3.77	0.0745			
4.00	0.0820*	0.0783	0.0037	
4.37	0.0877			1.40
6.00	0.132*	0.117	0.015	
7.23	0.163			1.38
7.80				1.36
8.00	0.186*	0.156	0.030	
9.51	0.229			1.34
10.00	0.245*	0.196	0.049	
11.13	0.280			1.31
13.05	0.347			1.30
15.00	0.410*	0.294	0.116	
15.55	0.442			1.30
19.04	0.572			1.28
20.00	0.604*	0.390	0.214	
23.41	0.749			1.26
25.00	0.800*	0.487	0.313	
27.22	0.901			1.25
30.00	1.008*	0.579	0.429	
31.37	1.05			1.25

\* = smoothed value taken from graph



Figure 13. Thermal Conductivity of Copper + 0.127% Iron Alloy

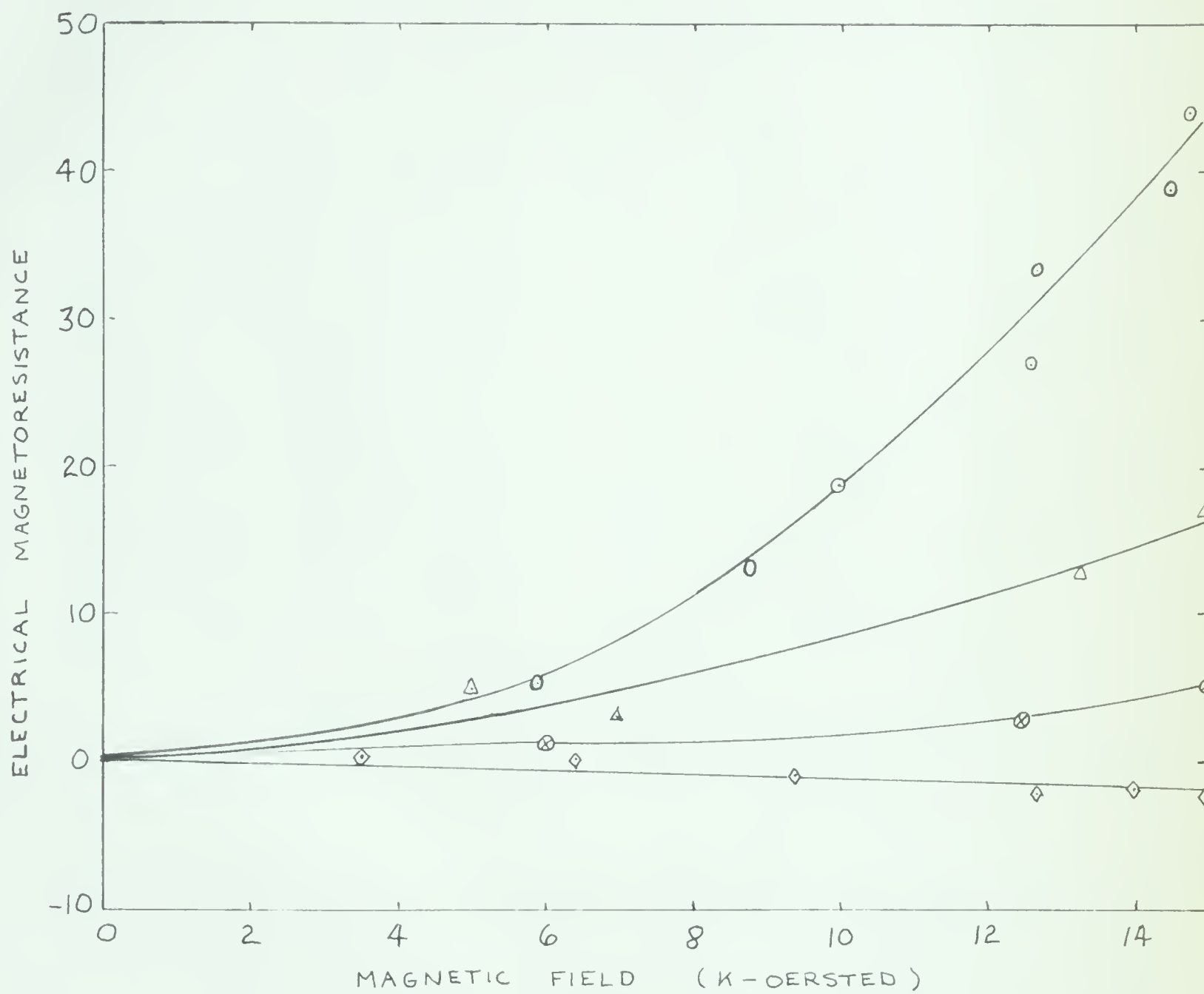




Electrical and Thermal Magnetoresistance  
of Copper and Copper-iron Alloys



Figure 14 . Electrical Magnetoresistance at 2 °K



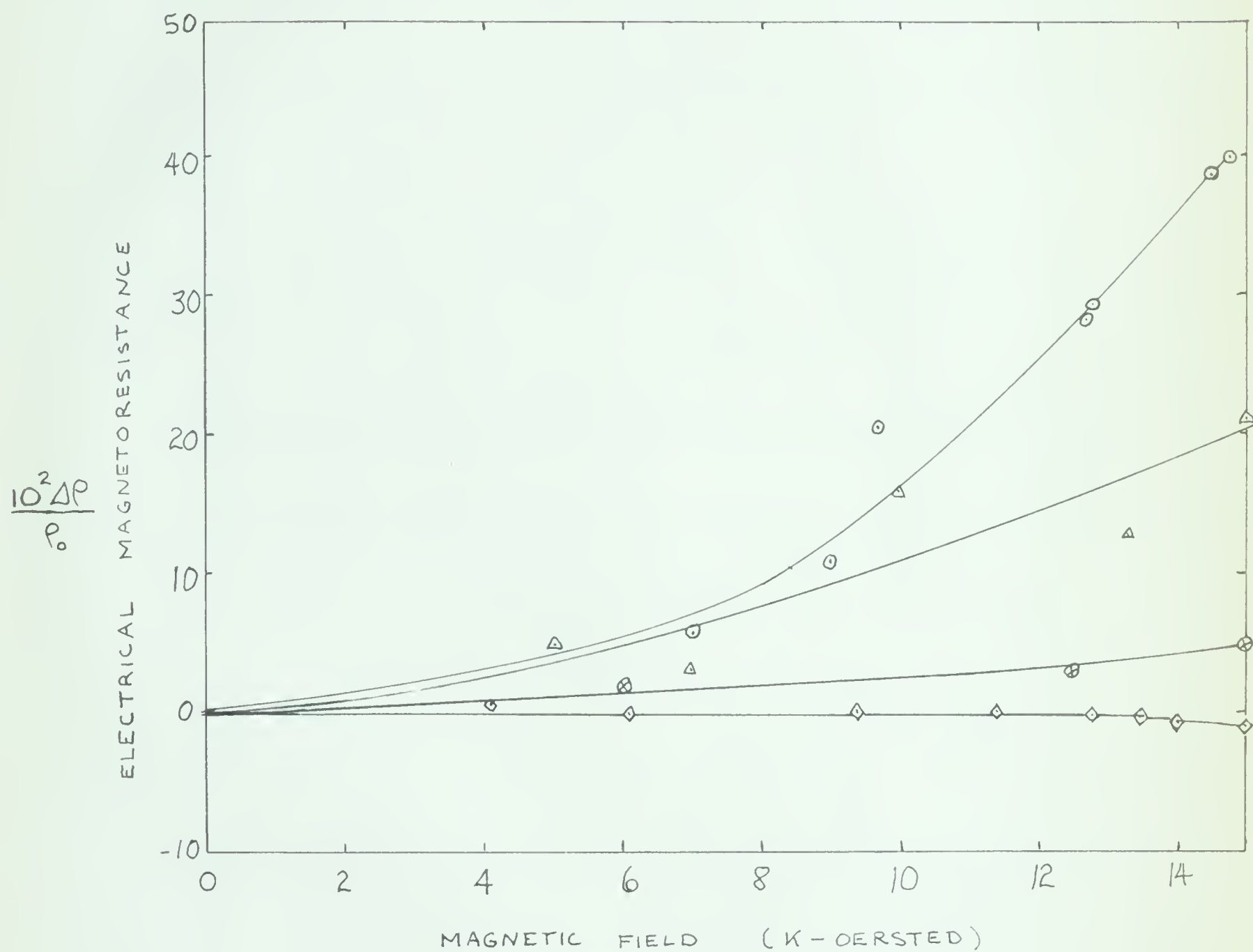
Legend:

- Pure copper
- △ 0.0013 % iron
- ⊗ 0.015 % iron
- ◇ 0.127 % iron





Figure 15 . Electrical Magnetoresistance at 42°K



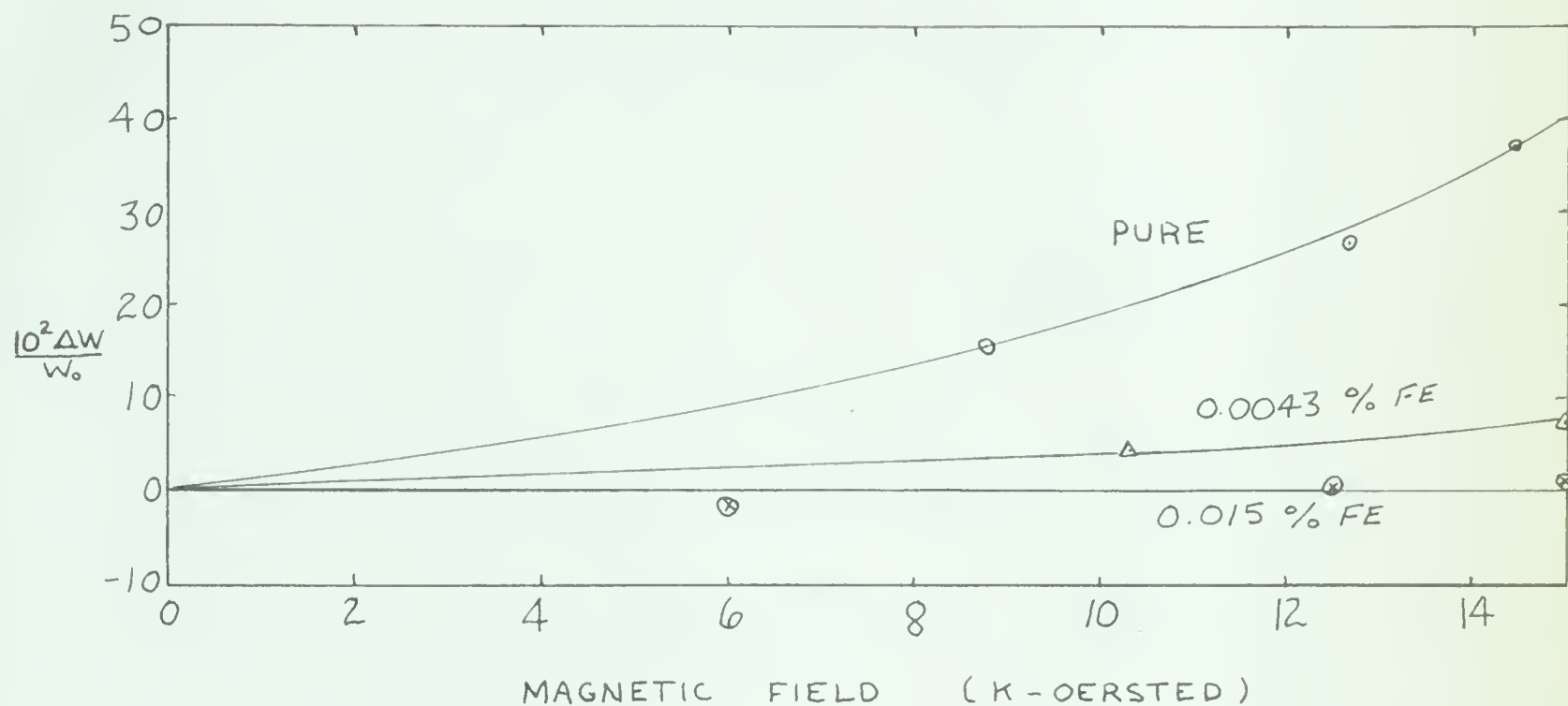
Legend:

- $\circ$  Pure copper
- $\Delta$  0.0043% iron
- $\otimes$  0.015% iron
- $\diamond$  0.127% iron



Figure 16 . Thermal Magnetoresistance

1) at 2 °K



2) at 4.2 °K

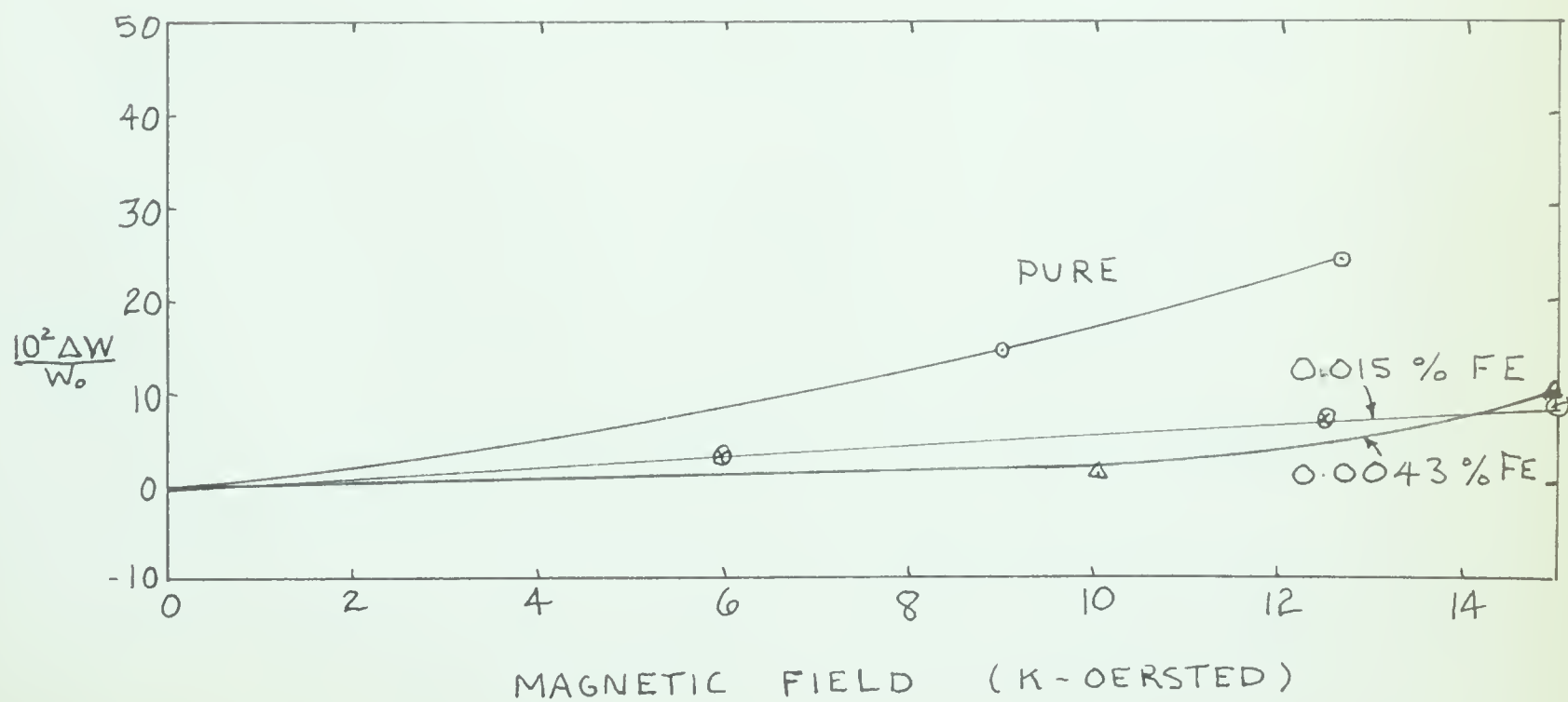
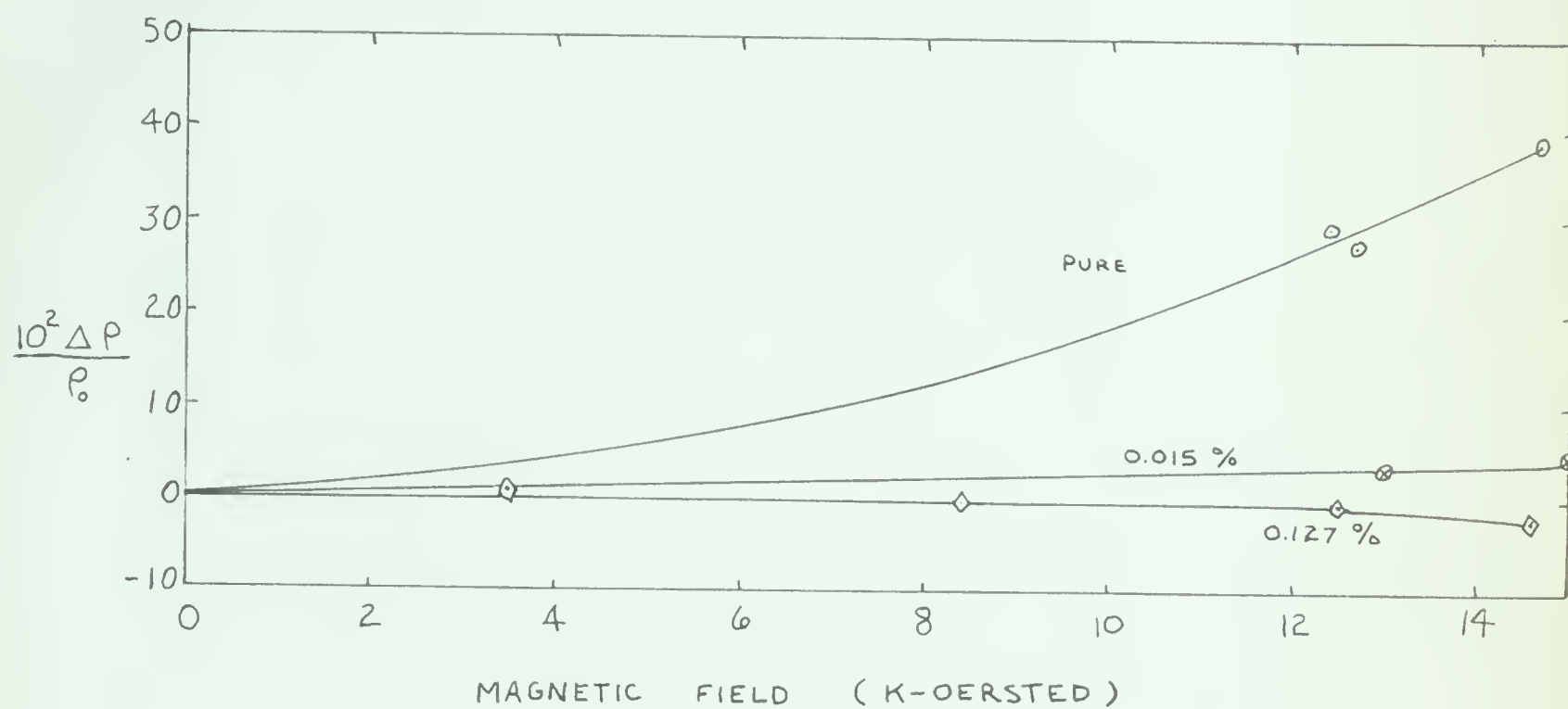




Figure 17. Magnetoresistance at 8 °K

## 1) Electrical



## 2) Thermal

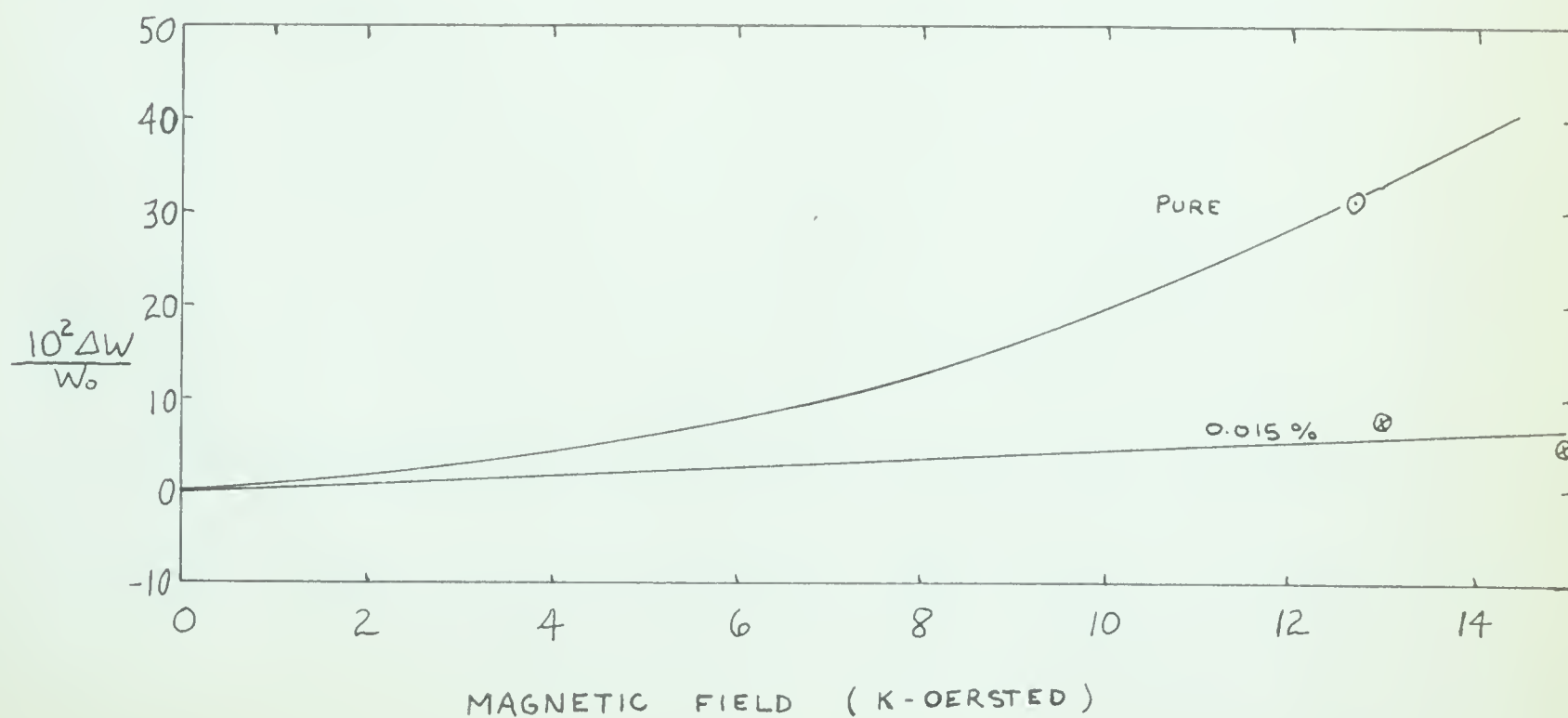
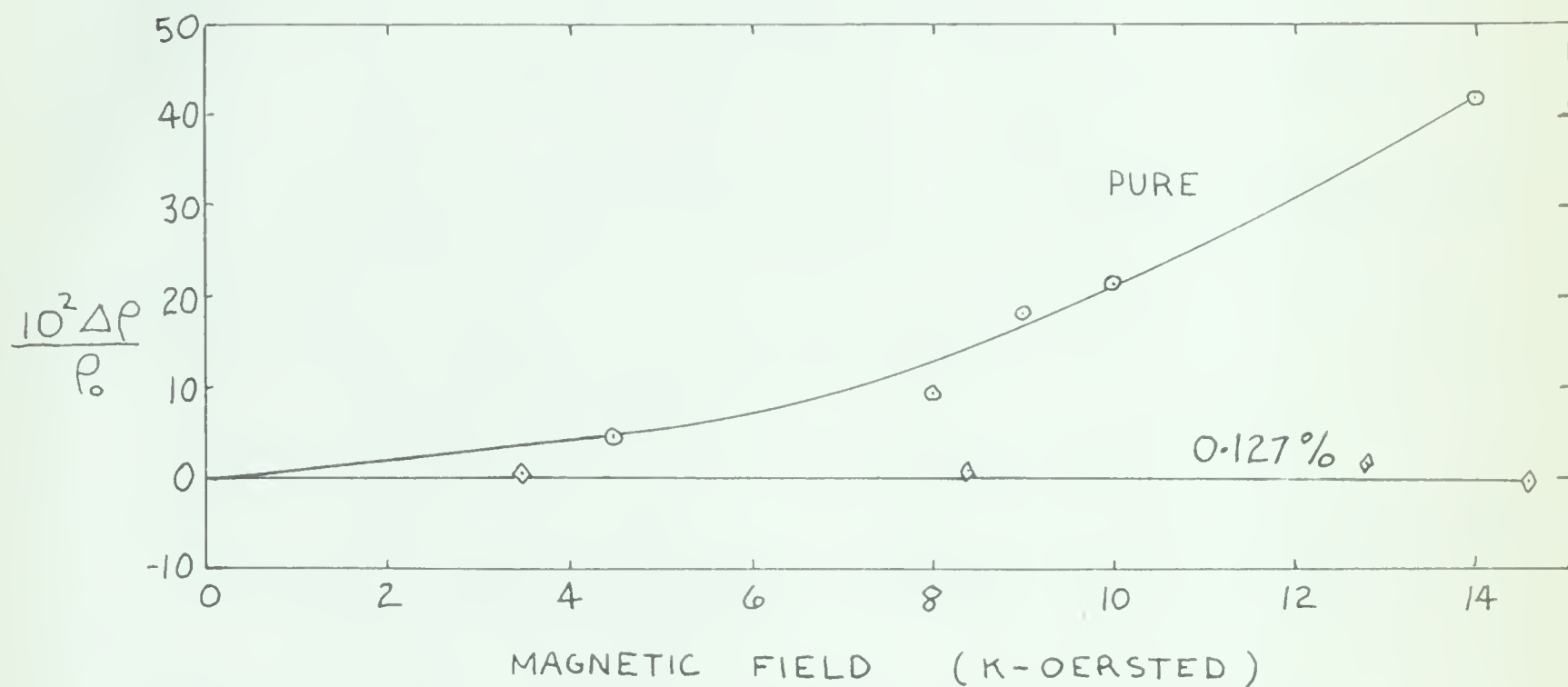




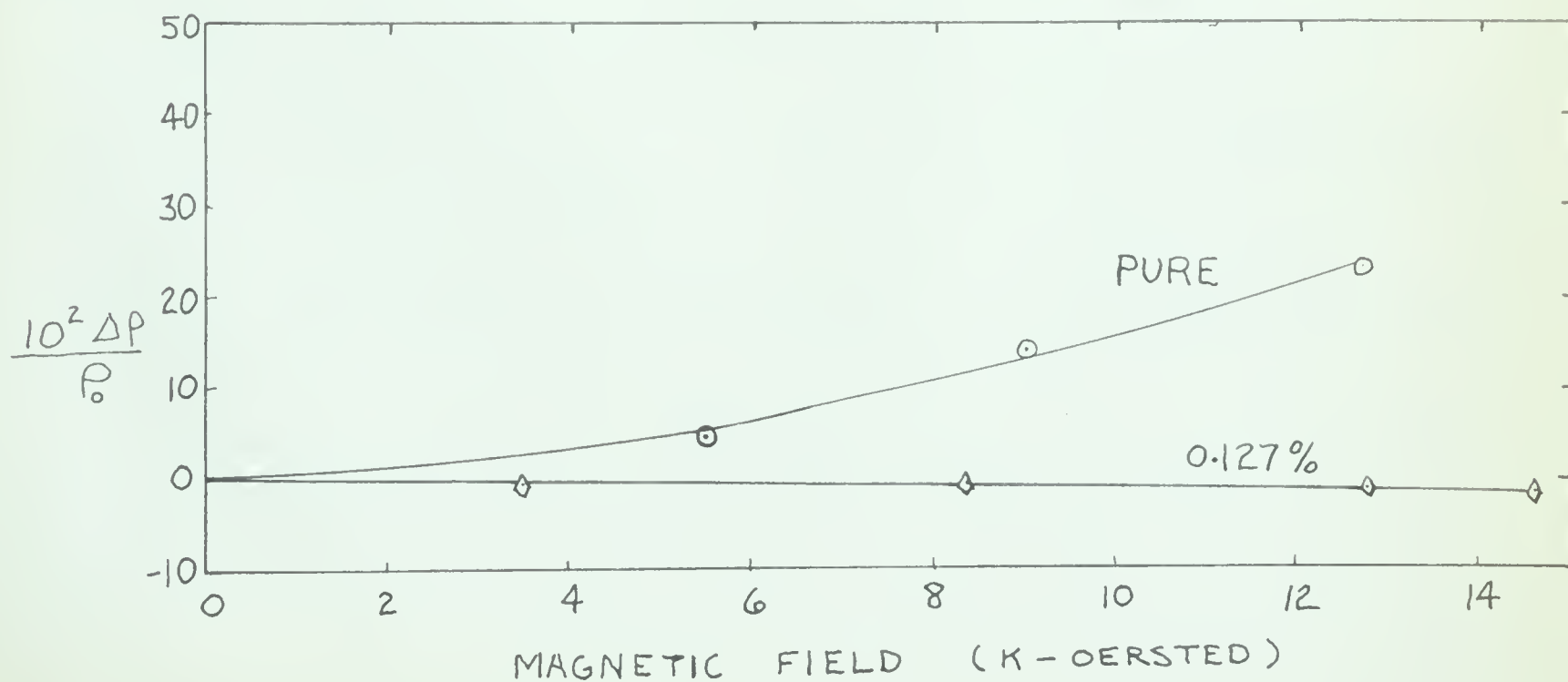


Figure 18 . Electrical Magnetoresistance

1) at 20 °K



2) at 30 °K





### 3.2 Conclusions

The thermal conductivity of these alloys has been measured and the electron thermal conductivity,  $k_e$ , has been calculated using the relation

$$k_e = (A/T - 7.1 \times 10^{-6} T^{2.4})^{-1}$$

The lattice thermal conductivity was deduced assuming that the electron and lattice conductivities are additive so that

$$k_g = k - k_e$$

where  $k$  is the total measured thermal conductivity,

and  $k_g$  is the lattice conductivity. The lattice conductivity shown in Figure 12 and 13 is found to increase as the square of the absolute temperature below 15 °K.

Table - Summary

Sample	$\rho_{295}$ $10^{-6}$ -cm.	$\rho_4$ $10^{-6}$ -cm.	$k_o/T$ w/cm-deg <sup>2</sup>	$d$ w/cm-deg <sup>3</sup>	$D$ cm-deg <sup>3</sup> /w
Pure	1.72	0.0126			
.0043%	1.72	0.0411			
0.015%	1.96	0.167	.155	$3.0 \times 10^{-3}$	333
0.127%	2.95	1.40	.0195	$4.9 \times 10^{-4}$	2040

The values of the scattering coefficient,  $D = 1/d$ , where  $k_g = dT^2$ , deduced here are higher than those of White (1962) but show a similar trend, increasing as the iron concentration increases. Since scattering by dislocations is proportional to  $1/T^2$  also, our high values of  $D$  may be due to a high density of dislocations even in these annealed specimens.



The electrical and thermal magnetoresistance ( Figures 14 to 18 ) is observed to decrease with increased amount of solute. Wilson and Sondheimer (1947) have shown theoretically that the lattice conductivity is unaltered in a magnetic field. One may write  $k_H = L\sigma_H T + k_g$ . In general the Lorenz number,  $L$ , is not independent of the magnetic field ( Wilson and Sondheimer (1947)), but plotting  $k_H$  versus  $\sigma_H T$  should yield information regarding its behavior. In the alloys however the variation of the electrical and thermal conductivity in the magnetic field is small and without more information about  $k_g$  the value of the Lorenz number could not be deduced. The Lorenz number for pure copper using the above equation was  $2.3 \times 10^{-8}$  watt-ohm/deg<sup>2</sup> (  $\pm 8 \%$  ). The theoretical value is  $2.45 \times 10^{-8}$  watt-ohm/deg<sup>2</sup>.

The expected change in the thermal conductivity corresponding to the observed minimum in the electrical resistivity has not been detected. This change would occur in the electron component of the thermal conductivity but in alloys the electron and lattice conductivities become comparable and for this reason the size of the anomaly in the total measured thermal conductivity,  $k = k_e + k_g$ , would be approximately one-half the size of the electrical resistivity minimum. Increasing the size of the minimum ( to 20 or 30 per cent ) might make the effect observable on the total conductivity; however the small solid solubility of iron in copper is the ultimate restriction on the size of the electrical resistivity minimum that can be obtained.





We found the electrical magnetoresistance of our pure copper to be 45 per cent when the magnetic field is 15 k-oersted. Gerritsen (1953) using a specimen of slightly lower residual resistance obtained a magnetoresistance of 83 per cent at 20 k-oersted. For very pure copper the magnetoresistance has been found as high as 250 per cent at 12 k-oersted (Chambers (1956)). Our pure copper showed no minimum in the electrical resistivity and the amount of impurity was insignificant.

Bailyn ( private communication ) has suggested that if the external field has the same effect as the internal magnetic field used as a model in his spin scattering theory for dilute alloys the resistivity would be decreased. This would explain our observations on the electrical and thermal magnetoresistivities.

A useful summary of the measurements on the transport properties of dilute alloys of noble metals with transition metals is given by Gerritsen (1959). The electrical magnetoresistance of many of these alloys has been measured but the thermal magnetoresistance has not. The gold-manganese alloys exhibit large, negative, electrical magnetoresistances and the Lorenz number could possibly be derived by measuring the thermal magnetoresistance. In general, the behavior of the Lorenz number in a magnetic field can be deduced only if the alloys have large thermal and electrical magnetoresistances. Since the solute concentration greatly affects the transport properties it is wise to choose alloy systems with high solid solubility.





## APPENDIX

Sample Calculation

For the copper-iron alloy containing 0.127% iron the constants were

$$T_o/P_o = 0.1130 \text{ } ^\circ\text{K/cm. } (\pm 0.3\%)$$

$$\ell/A = 16.1 \text{ cm.}^{-1} (\pm 1.0\%)$$

$$c = 1.620 \times 10^{-9} \text{ volt/ohm-cm.}$$

The temperature was determined

$$P_v = 19.9 \text{ cm. using the 1958 He}^4 \text{ scale } T_v = 3.063^\circ\text{K}$$

$$P = 27.10 \text{ cm. } T = P(T_o/P_o) \left( \frac{1+\Delta}{1+\Delta_o} \right) = 3.062 \text{ } ^\circ\text{K}$$

For the electrical resistivity measurements were

$$\text{Current } I = 100 \text{ m.a. } (\pm 0.5\%)$$

$$\text{Deflection } 2d = 70.05 \text{ cm. } (\pm 0.4\%)$$

$$\text{Feedback resistance } R_f = 20 \text{ ohms } (0.05\%)$$

$$\text{Resistivity } \rho = \frac{cR_f 2d}{I(\ell/A)} = 1.41 \times 10^{-6} \text{ ohm-cm. } (\pm 2.0\%)$$

For the thermal conductivity measurements were

$$\text{Specimen heater voltage } V_h = 0.2985 \text{ volts}$$

$$\text{Specimen heater current } V_s = 0.3082 \text{ volts}$$

$$\text{Series resistance } R = 400 \text{ ohms}$$

$$P_k = 28.65 \text{ cm. } (\pm 0.2\%)$$

$$\delta_p = 0.512 \text{ cm. } (\pm 0.8\%)$$



$$T_K = p_k(T_o/P_o) \left( \frac{1+\Delta}{1+\Delta_o} \right) = 3.235^\circ\text{K} (\pm 0.5\%)$$

$$\delta_T = p \left\{ (T_o/P_o) \left( \frac{(1+\Delta)^2}{1+\Delta_o} \right) + \beta \right\} = 0.0580^\circ\text{K} (\pm 0.8\%)$$

$$T_{k)\text{average}} = 3.264^\circ\text{K} (\pm 0.8\%)$$

$$\text{Heater power } \dot{Q} = V_h V_s / R = 0.2300 \text{ mw. } (\pm 0.8\%)$$

$$\text{Thermal Conductivity } k = \frac{\dot{Q} (1/A)}{\delta T} = 0.0639 \frac{\text{W}}{\text{cm-}^\circ\text{K}} (\pm 2.6\%)$$



## BIBLIOGRAPHY

- Adler J., The Thermoelectric Power of Sodium, M. Sc. Thesis, University of Alberta, (1960)
- Bailyn M., Research Report 029-B000-P1 Westinghouse (1961)
- Bailyn M., private communication (1962)
- Bethe H., Nature 127, 336 (1931)
- Bloch F., Z. Physik, 59, 208 (1930)
- Chambers R. G., Proc. Roy. Soc., 238, 344 (1956)
- Chari M. S. R., Proc. Phil. Soc., 78, 1360 (1961)
- Chari M. S. R. and deNobel J., Physica 25, 60 (1959)
- Dauphinee T. and Woods S. B., Rev. Sci. Inst. 26, 693 (1955)
- Fenton E. W., The Lorenz Numbers of Gold and Silver, M. Sc. Thesis, University of Alberta, (1962)
- Gerritsen A. N., Physica 19, 61 (1953)
- Gilmont R., Anal. Chem. 23, 157 (1951)
- Gold A. V., MacDonald D. K. C., Pearson W. B. and Templeton I. M., Phil. Mag. 5, 765 (1960)
- Kasuya T., Prog. Theo. Phys. 22, 227 (1959)
- Klemens P. G., Aust. J. Phys. 7, 57 (1954)
- Korringa J. and Gerritsen A. N., Physica 19, 457 (1953)
- MacDonald D. K. C., J. of Scientific Instruments, Vol. 24, No. 9 (1947)
- MacDonald D. K. C., and Sarginson K., Rep. Prog. Phys. 15, 249 (1952)
- Massalski T. B. and King H. W., Proc. Int'l Conf. on the Fermi Surface 290, (1960)
- Olsen R. and Rodriguez S., Phys. Rev. 108, 1212 (1957)
- Pearson W. B., Phil. Mag. 46, 911 (1955)
- Pippard A. B., Trans. Phil. Soc. A 250, 325 (1957)
- Rogers J. S., The Lorenz Number of Aluminum, M. Sc. Thesis University of Alberta (1962)
- Tainsh R. J. and White G. K., J. Chem. Phys. of Solids 23, 1329 (1962)



Wilson A. H., The Theory of Metals, 2nd ed., Cambridge University Press (1953)

White G. K. and Woods S. B., Can. J. Phys. 33, 58 (1955)

Ziman J. M., Electrons and Phonons, Oxford University Press (1960).

Sondheimer E.H. and Wilson A.H., Proc.Roy. Soc. A190 435 (1947)







**B29806**